

## Test for maximal $P$ , maximal $C$ violation in $e^-e^+$ collisions from beam-referenced spin-correlation functions

Charles A. Nelson

*Department of Physics, State University of New York, Binghamton, New York 13902-6000*

(Received 6 September 1990)

For unpolarized beams in  $e^-e^+$  collisions at the  $Z^0$ , beam-referenced spin-correlation functions for the production-decay sequence  $e^-e^+ \rightarrow Z^0 \rightarrow \tau_1^- \tau_2^+ \rightarrow (h_1^- \nu)(h_2^+ \bar{\nu})$  can be easily derived using the helicity approach. For  $\tau_1^- \rightarrow \pi_1^- \nu$ , for example, this reaction is analyzed relative to the final  $\pi_1^-$  momentum vector. The most interesting result is an azimuthal correlation function  $I(\phi_e, \phi)$  where the azimuthal angles are defined relative to the final  $\pi_1^-$ .  $I(\phi_e, \phi)$  allows one to simply test for maximal  $P$ , maximal  $C$  violation in the  $Z^0 \rightarrow \tau_1^- \tau_1^+$  coupling. For  $e^-e^+$  collisions in the  $\Upsilon$  or  $J/\psi$  regions,  $I(\phi_e, \phi)$  can be used to test for a complex phase in the  $\gamma^* \rightarrow \tau^- \tau^+$  coupling. Previously it was shown that the measurement of the energy correlation function  $I(E_A, E_B)$  for  $Z^0 \rightarrow \tau_1^- \tau_1^+ \rightarrow A^- B^+ X$  determines independently the fundamental parameters  $\sin^2\theta_W$ , the  $\tau$  Michel parameters, and for hadronic  $\tau$  decays the analogous chirality parameter  $\xi_A$  which tests for right-handed currents. Now by referencing this energy correlation function to the incident  $e^-$  beam direction, the associated ideal statistical errors for these parameters for the case of hadronic  $\tau$  decays are reduced only by about 25%.

### I. INTRODUCTION

At the CERN  $e^+e^-$  collider LEP in four high-precision experiments,<sup>1-4</sup> many  $\tau^- \tau^+$  events are being produced by unpolarized  $e^-e^+$  collisions<sup>5</sup> in the  $Z^0$  mass region. Many  $\tau^- \tau^+$  events are also being produced in the  $\Upsilon$  region in the ARGUS (Ref. 6) and CLEO (Ref. 7) detectors. There is also a strong interest in the physics community in the construction of a high-luminosity  $e^-e^+$  collider near the  $\tau^- \tau^+$  threshold to produce a high-statistics sample of  $\tau^- \tau^+$  events (the so-called  $\tau$  charm factory).<sup>8</sup>

It is very important that these experiments *not only* make high-precision measurements of fundamental parameters such as  $\sin^2\theta_W$ , assuming that the  $\tau$  is an orthodox sequential heavy lepton, *but also systematically search* for new phenomena outside the standard model such as violations of lepton universality and right-handed currents in  $\tau$  decays, and observable complex phases in the  $Z^0 \rightarrow \tau^- \tau^+$  and  $\gamma^* \rightarrow \tau^- \tau^+$  couplings. Previously,<sup>9-11</sup> it was shown<sup>10</sup> that measurement of the energy-correlation function  $I(E_A, E_B)$  for the decay sequence

$$Z^0 \rightarrow \tau^- \tau^+ \begin{cases} \rightarrow B^+ X \\ \rightarrow A^- X \end{cases} \quad (1.1)$$

determines independently the fundamental parameters  $\sin^2\theta_W$ , the  $\tau$  (Ref. 12) Michel parameters for  $\tau^- \rightarrow l^- \nu \bar{\nu}$ , where  $l = \mu$  or  $e$ , and for hadronic  $\tau$  decays  $\tau^- \rightarrow h^- \nu$  the analogous chirality parameter  $\xi_h$ , which tests for possible right-handed currents. This parameter

$$\xi_h = \frac{|g_L|^2 - |g_R|^2}{|g_L|^2 + |g_R|^2} \quad (1.2)$$

has the value  $\xi = \pm 1$ , respectively, for a pure  $V \mp A$  coupling in  $\tau^- \rightarrow h^- \nu$ .

In this paper we generalize this analysis<sup>10</sup> and consider the production-decay sequence

$$e^-e^+ \rightarrow Z^0 \rightarrow \tau_1^- \tau_2^+ \rightarrow (h_1^- \nu)(h_2^+ \bar{\nu}) \quad (1.3)$$

The treelike structure of this process is illustrated in Fig. 1 for the  $\{\pi_1^- \pi_2^+\}$  final state. A central idea is to analyze this reaction [Eq. (1.3)] relative to the final  $\pi_1^-$  momentum vector. The standard reference system, therefore, is that shown in Fig. 2. Note that the final  $\pi_2^+$  momentum has been used to specify the positive  $x$  half-plane.

The energy correlation function  $I(E_1, E_2)$ , which was studied earlier, exploited the  $\tau$  spin correlation in the sequential decay starting from the  $Z^0$ . Because the initial  $e^-$  and  $e^+$  beams are unpolarized, it is natural for this reaction to work backward from the observed final state in the analysis of the complete process. So, as shown in

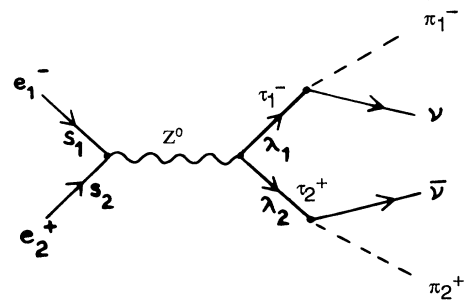


FIG. 1. Illustration of the treelike structure of the helicity amplitude description of the production-decay sequence  $e^-e^+ \rightarrow Z^0 \rightarrow \tau_1^- \tau_2^+ \rightarrow (\pi_1^- \nu)(\pi_2^+ \bar{\nu})$ .

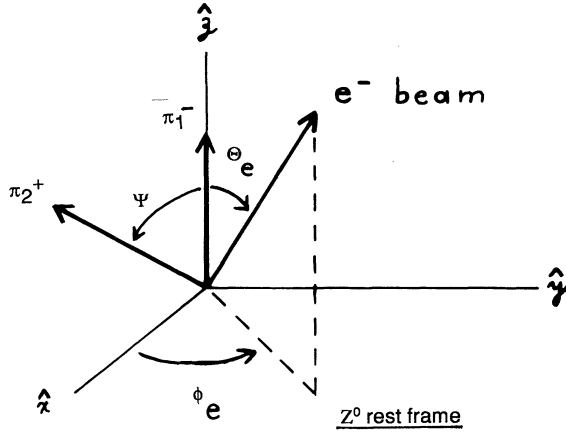


FIG. 2. Angles describing the distribution of the incident  $e^-$  beam relative to the final  $\pi^-$  and  $\pi^+$  momentum directions in the  $Z^0$  rest frame. The  $\pi^+$  momentum specifies the  $\phi_e = 0$  half-plane.

Fig. 2, we now include the direction of the incident  $e^-$  beam in this standard reference system. This references the earlier-considered  $\tau$  spin correlation to the initial  $e^-$  beam, and so we call the resulting correlation functions “beam-referenced spin-correlation functions” (BRSC). Actually, these are nothing more than angular distributions. However, the name “BRSC” is appropriate, for the useful variables are indeed those which occur naturally in a final-state spin-correlation function ( $E_1, E_2, \phi$ ) and in the referencing of it to the initial beam direction ( $\theta_e, \phi_e$ ) as shown in Fig. 2.

The paper has been organized so that an interested reader can select those parts he wishes to read, while omitting other parts. The headings of the various sections and appendixes clearly indicate their respective contents.

Section II contains what appears to be the most interesting result of this analysis. There is an azimuthal correlation function  $I(\phi_e, \phi)$  where the azimuthal angles are relative to the final  $\pi_1^-$ , which allows one to simply test for maximal  $P$ , maximal  $C$  violation in the  $Z^0 \rightarrow \tau^- \tau^+$  coupling. For  $e^- e^+$  collisions in the  $\Upsilon$  and  $J/\psi$  regions, the test is for a complex phase in the  $\gamma^* \rightarrow \tau^- \tau^+$  coupling. Compare the  $CP$  tests in Refs. 13 and 14.

In Sec. III we return to a deductive organization for the rest of the paper. In this section we explain the kinematics of the production-decay sequence [Eq. (1.3)].

In Sec. IV, using the helicity formalism, we derive the full beam-referenced spin-correlation function  $I(\theta_e, \phi_e, E_1, E_2, \phi)$  for

$$e^- e^+ \rightarrow Z^0 \rightarrow \tau_1^- \tau_2^+ \rightarrow (\pi_1^- \nu) (\pi_2^+ \bar{\nu}). \quad (1.4)$$

The helicity approach is both convenient, simple, and powerful in describing reactions such as that shown in Fig. 1. Very useful kinematic variables appear from the start in this approach, in spite of the need to be careful due to the missing  $\nu$  and  $\bar{\nu}$  momenta.

Section V contains the analytic expressions for the azimuthal correlation function  $I(\phi_e, \phi)$  discussed earlier in Sec. II.

Section VI shows that there is a simple  $\xi^S$  substitution rule which directly converts any BRSC for  $\{\pi_1^- \pi_2^+\}$  [Eq. (1.4)] to that for  $\{h_1^- h_2^+\}$  [Eq. (1.3)].

In Sec. VII the ideal statistical errors for a  $10^7$   $Z^0$  event sample for the determination of  $\sin^2 \theta_W$  and of the chirality parameters  $\xi_h$  are compared between those obtained when one uses the full BRSC function  $I(\theta_e, \phi_e, E_1, E_2, \phi)$ , and those obtained when one uses the simpler energy-correlation function  $I(E_1, E_2)$ .

The principal conclusions are listed in Sec. VIII.

Additional material which will be of interest to certain readers is contained in the appendixes.

We stress that the information in this paper is limited. Experimental information (resolutions, biases, systematic errors, etc.) and additional theoretical information (radiative corrections, etc.) need to be systematically included. This can be best done by  $\tau$ -pair Monte Carlo simulations.<sup>15</sup>

## II. TEST FOR MAXIMAL $P$ , MAXIMAL $C$ VIOLATION

In this section we (i) define what we mean by “maximal  $P$ , maximal  $C$ ” violation in the  $Z^0 \rightarrow \tau^- \tau^+$  decay amplitude, and (ii) explain the striking signature in an azimuthal correlation function  $I(\phi_e, \phi)$  for other than maximal  $P$ , maximal  $C$  violation in  $Z^0 \rightarrow \tau^- \tau^+$  decay.

Let  $T(\lambda_1 \lambda_2)$  be the helicity amplitude which describes the decay  $Z^0 \rightarrow \tau^- \tau^+$ , where  $\lambda_1, \lambda_2$  are the respective helicities for the  $\tau_1^-$  and  $\tau_2^+$ . If either  $P$  invariance or  $C$  invariance were exact symmetries in  $Z^0 \rightarrow \tau^- \tau^+$  decay, then

$$T(+ -) = T(- +). \quad (2.1)$$

In contrast, in the standard model at Born level, the  $Z^0 \rightarrow \tau^- \tau^+$  helicity amplitudes in the Jacob-Wick<sup>16</sup> phase convention are (see Appendix A)

$$T(- +) = \frac{1}{\sqrt{2}}(M + 2\bar{P}r), \quad (2.2a)$$

$$T(+ -) = \frac{1}{\sqrt{2}}(M - 2\bar{P}r), \quad (2.2b)$$

$$T(++ ) = T(-- ) = m, \quad (2.2c)$$

with  $M = Z^0$  mass,  $m = \tau$  mass, and  $\bar{P} =$  magnitude of a final  $\tau$  momentum in the  $Z^0$  rest frame. The  $r$  parameter

$$r = \frac{a}{v} = \frac{1}{(1 - 4 \sin^2 \theta_W)} \quad (2.3)$$

$$\simeq 12.5 \text{ for } \sin^2 \theta_W = 0.23. \quad (2.4)$$

The form of the standard-model equation (2.2) does not violate  $CP$  invariance. In general, if  $CP$  invariance is assumed,

$$T(++ ) = T(-- ), \quad (2.5)$$

but  $T(+ -)$  and  $T(- +)$  are not related. These various

TABLE I. Relations among the  $Z^0 \rightarrow \tau^- \tau^+$  helicity amplitudes due, respectively, to  $CP$ ,  $P$ , or  $C$  invariance.

If $Z^0 \rightarrow \tau_1^- \tau_2^+$	Then
$CP$ invariant	$T(++)=T(--)$
$P$ invariant	$T(+-)=T(-+), T(++)=(T--)$
$C$ invariant	$T(+-)=T(-+)$

symmetry relations are tabulated in Table I.

The Born-level standard-model (SM) amplitudes equations (2.2a) and (2.2b) do have another property, however, and it is the one we are interested in here: Both  $T(-+)$  and  $T(+ -)$  have the same phase. Empirically, one sees that this property can be simply stated in terms of the measurable  $Z^0 \rightarrow \tau^- \tau^+$  decay intensity parameter

$$\kappa' \equiv \frac{2}{\mathcal{N}} \text{Im}[T(+ -)T^*(- +)], \quad (2.6)$$

where the overall normalization factor is

$$\mathcal{N} = \sum |T(\lambda_1, \lambda_2)|^2 \rightarrow (1 + r_\tau^2) \mathcal{M}^2, \quad (2.7)$$

where the arrowed result is the Born-term value in the standard model. We will soon explain how the value of  $\kappa'$  can be simply measured from the azimuthal correlation function  $I(\phi_e, \phi)$ . We define maximum  $P$ , maximum  $C$  violation to mean that the amplitudes  $T(+ -)$  and  $T(- +)$  are *unequal, but with the same phase*; that is,  $\kappa' \neq 0$ . Even though  $\kappa' = 0$  follows from the Born-level  $Z^0 \rightarrow \tau^- \tau^+$  coupling in the standard model, it is very important to test whether this is, indeed, true in nature. In an effective Hamiltonian framework, the origin of such a violation would be a violation of  $T$  invariance, i.e., a violation time-reversal invariance, *when* a first-order perturbation in a Hermitian Hamiltonian can be regarded as reliable. Consequently, to relate  $\kappa' \neq 0$  and  $T$  noninvariance requires further theoretical or empirical information on the scale of the effective Hermitian Hamiltonian. In particular,  $\kappa' \neq 0$  could be due to a strong-interaction higher-order effect in a Hamiltonian framework such as could be induced by a strongly interacting Higgs sector or from the existence of supersymmetric particles. In the literature<sup>13,14,17</sup> on  $CP$  violation and on  $T$  violation in the kaon and hyperon systems, such effects are sometimes referred to as unitarity corrections, or final-state corrections. Here the process is  $Z^0 \rightarrow \tau^- \tau^+$ , and so a strong-interaction higher-order effect would be a signal of new physics.

In the case of  $CP$  violation, one can frequently define  $CP$ -even and  $CP$ -odd combinations of observables for the reaction of interest and the  $CP$ -conjugate reaction, and thereby separate fundamentally  $CP$ -violating phenomena from that due to a strong-interaction higher-order effect. In contrast, here the time-reversal operation relates the decay process  $Z^0 \rightarrow \tau^- \tau^+$  to the formation process  $\tau^- \tau^+ \rightarrow Z^0$ , which is not experimentally available. Consequently, it is not obviously helpful here to define  $T$ -even and  $T$ -odd combinations of analogous observables for the decay and formation reactions. If  $\tau$ - $e$  universality is assumed, this can be done, and certainly if a candidate effect is observed in one, e.g.,  $Z^0 \rightarrow \tau^- \tau^+$ , it should be

looked for using polarized initial beams in the other,  $e^-e^+ \rightarrow Z^0$ .

### A. Signature for $\kappa' \neq 0$

Later in this paper the full beam-referenced spin-correlation function  $I(\theta_e, \phi_e, E_1, E_2, \phi)$  will be derived for the production-decay sequence

$$e^-e^+ \rightarrow Z^0 \rightarrow \tau_1^- \tau_2^+ \rightarrow (h_1^- \nu)(h_2^+ \bar{\nu}).$$

However, the simpler azimuthal correlation function

$$I(\phi_e, \phi) = L(\phi_e, \phi) [1 + \kappa' R(\phi_e, \phi)], \quad (2.8)$$

in the  $Z^0$  rest frame, is almost as sensitive to  $\kappa'$ . See Figs. 2 and 3, respectively, for the definition of the two azimuthal angles. Figure 2 shows that  $\phi_e$  is the azimuthal angle of the incident  $e^-$ , in the  $Z^0$  rest frame, with  $\pi^-$  moving in the positive  $z$  direction. The  $\pi^+$  momentum vector specifies the positive  $x$  half-plane.

The other angle  $\phi$  that appears in the azimuthal correlation function  $I(\phi_e, \phi)$  is the angle which was used in the  $\phi\phi$  parity test<sup>18</sup> for the  $\eta_c$ . There  $\eta_c \rightarrow \phi_1 \phi_2 \rightarrow (K^+ K^-)(K^+ K^-)$  and the angle  $\phi$  is simply the angle between the  $\phi_1 \rightarrow (K^+ K^-)$  and  $\phi_2 \rightarrow (K^+ K^-)$  decay planes in, for instance, the  $\eta_c$  rest frame. The one-dimensional decay distribution in the angle  $\phi$  provided a striking signature of the pseudoscalar nature of the  $\eta_c$  from around 18 events. So it is physically natural to introduce the analogous angle here, and indeed, again, the spin-correlation effect has a very striking behavior in the  $\phi$  variable.

Therefore, the angle  $\phi$  is the azimuthal angle between

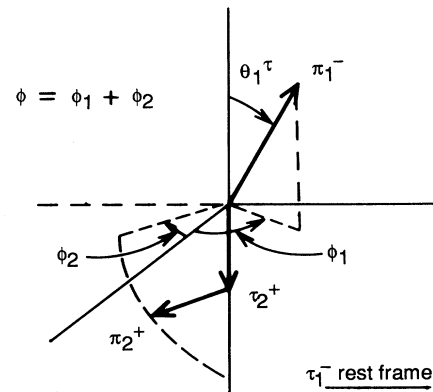


FIG. 3. Usual helicity angles  $\theta_1^-$  and  $\phi_1$  specifying the  $\pi_1^-$  momentum, in the  $\tau_1^-$  rest frame, with  $\tau_2^+$  moving in the negative  $z$  direction. The polar angle  $\theta_2^+$  for the  $\pi_2^+$  is defined analogously in the  $\tau_2^+$  rest frame. The azimuthal angles  $\phi_1$  and  $\phi_2$  are Lorentz invariant under boosts along the  $z$  axis. The sum  $\phi = \phi_1 + \phi_2$  is the angle between the  $\tau_1^-$  and  $\tau_2^+$  decay planes. Its cosine, i.e.,  $\cos\phi$ , is measurable [Eq. (3.15)]. The angles  $\theta_1^-$  and  $\theta_2^+$  are also measurable [see, respectively, Eqs. (3.5) and (3.9)].

the  $\tau^- \rightarrow \pi^- \nu$  and  $\tau^+ \rightarrow \pi^+ \bar{\nu}$  decay planes in the sequential decay

$$Z^0 \rightarrow \tau^- \tau^+ \begin{cases} \swarrow \pi^+ \bar{\nu} \\ \searrow \pi^- \nu \end{cases} \quad (2.9)$$

This angle  $\phi$  is displayed in Fig. 3 for the  $\tau^-$  rest frame, with the  $\tau^+$  moving in the negative  $z$  direction. The angle  $\phi$  is Lorentz invariant under boosts along the  $z$  axis of Fig. 3. In particular,  $\phi$  is also the opening angle between the  $\tau^-$  and  $\tau^+$  decay planes in the  $Z^0$  rest frame.

Kinematically,  $\cos\phi$  can be expressed, in the  $Z^0$  rest frame, in terms of the energies of the final  $\pi^-$  and  $\pi^+$ , and the opening angle  $\psi$  between them. This angle  $\psi$  is also shown in Fig. 2. [For the explicit formula for  $\cos\phi$ , see Eq. (3.16) below with Eqs. (3.6) and (3.9)]. As explained in detail in Sec. III because of the missing  $\nu$  and  $\bar{\nu}$  momenta, the empirical sign of the  $\sin\phi$  is not known. (From  $\cos\phi$  one knows only the magnitude of  $\sin\phi$ , but not whether  $\sin\phi$  is positive or negative). So, in the following figures, in order to use  $\phi$  and not  $\cos\phi$  as the variable, we have restricted  $\phi$  to the range  $0^\circ$ – $180^\circ$ . To us,  $\phi$  is the more convenient variable for plots, etc.

Figures 4 and 5 show<sup>19</sup> the Born-level contour plots of  $L(\phi_e, \phi)$  and  $R(\phi_e, \phi)$  for the case  $\tau^- \rightarrow \pi^- \nu$  and  $\tau^+ \rightarrow \pi^+ \bar{\nu}$ . Since we find  $L$  and  $R$  to both be periodic in  $\phi_e$  with a period of  $180^\circ$ , in the figures we have only shown  $\phi_e$  in the range between  $\pm 90^\circ$ .

We stress that  $L(\phi_e, \phi)$  is what is predicted at the Born level in the standard model for  $\sin^2\theta_W=0.23$ . By Eq.

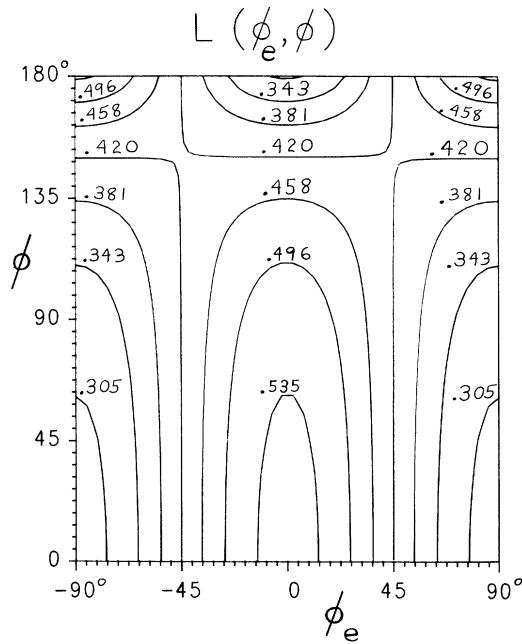


FIG. 4. For  $\tau^- \rightarrow \pi^- \nu$  and  $\tau^+ \rightarrow \pi^+ \bar{\nu}$ , the  $L(\phi_e, \phi)$  factor in the azimuthal correlation function  $I(\phi_e, \phi) = L(\phi_e, \phi)[1 + \kappa' R(\phi_e, \phi)]$ . Since  $I(\phi_e, \phi)$  is periodic in  $\phi_e$  with period of  $180^\circ$ , in this plot  $\phi_e$  ranges from  $-90^\circ$  to  $+90^\circ$ . Note that  $L(\phi_e, \phi)$  is symmetric about  $\phi_e = 0^\circ$ .

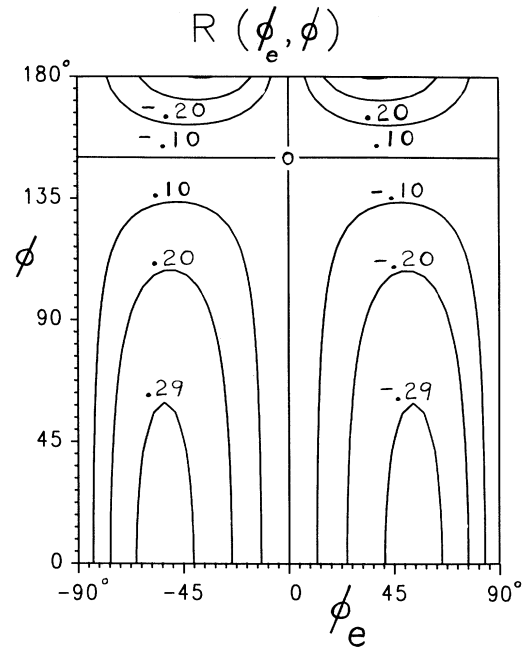


FIG. 5.  $R(\phi_e, \phi)$  term in the azimuthal correlation function for the  $\{\pi^- \pi^+\}$  spectrum. Note  $R$  is asymmetric about  $\phi_e = 0^\circ$ .

(2.8),  $R(\phi_e, \phi)$  is the “analyzing power” to measure  $\kappa'$ . In the standard model with no  $CP$ -violating phase in the lepton sector,  $\kappa' = 0$  at the Born level.

In Fig. 6 the  $K'$  distribution is shown where, instead of Eq. (2.8), one writes the azimuthal correlation function

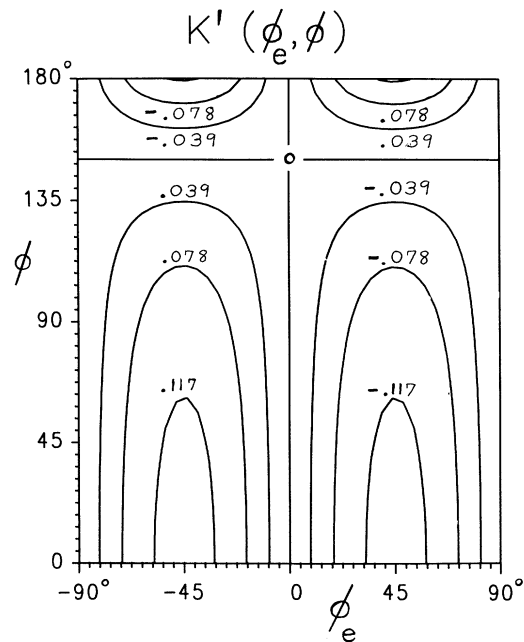


FIG. 6.  $K'(\phi_e, \phi)$  term in the azimuthal correlation function written as  $I(\phi_e, \phi) = L(\phi_e, \phi) + \kappa' K'(\phi_e, \phi)$  for the  $\{\pi^- \pi^+\}$  spectrum. Note that  $K'$  is asymmetric about  $\phi_e = 0^\circ$ .

in the form

$$I(\phi_e, \phi) = L(\phi_e, \phi) + \kappa' K'(\phi_e, \phi), \quad (2.10a)$$

and so

$$R(\phi_e, \phi) = \frac{K'(\phi_e, \phi)}{L(\phi_e, \phi)}. \quad (2.10b)$$

Note that  $L$  is symmetric about the  $\phi_e = 0$  axis, whereas both  $R$  and  $K'$  are antisymmetric.

Explicit expressions for  $L$  and  $K'$  are given, respectively, by Eqs. (5.2a) and (5.2b) in Sec. V. Specifically,  $L(\phi_e, \phi)$  contains terms in the angle  $\phi_e$  which are constant, vary as  $\cos\phi_e$ , and vary as  $\cos 2\phi_e$ , whereas,  $K'(\phi_e, \phi)$  varies as  $\sin 2\phi_e$  since

$$K'(\phi_e, \phi) = \frac{32\pi}{3} \sin 2\phi_e K'(\phi), \quad (2.11a)$$

where

$$K'(\phi) = \frac{1}{0.622} L(\phi) R(\phi), \quad (2.11b)$$

with  $L(\phi)$  and  $R(\phi)$  as shown, respectively, in Figs. 7 and 8. [Here  $(0.662)^{-1} \simeq 3(5/2\pi)^2$ .]

This antisymmetry for  $K'(\phi_e, \phi)$  about the  $\phi_e$  axis is as would be expected from a simple symmetry argument for a triple-product correlation  $(\mathbf{p}_{\pi^-} \times \mathbf{p}_{\pi^+}) \cdot \mathbf{p}_e$ : As shown in Fig. 9, by time-reversal invariance and rotational invariance, such antisymmetric in  $\phi_e$  terms must be absent if the decay is due to a Hermitian effective Hamiltonian in lowest order.

This symmetry of  $I(\phi_e, \phi)$  with respect to the  $\phi_e = 0$  axis enables a simple one-dimensional display of this azimuthal correlation. For events with  $\phi_e$  in the  $0^\circ - 90^\circ$ , we

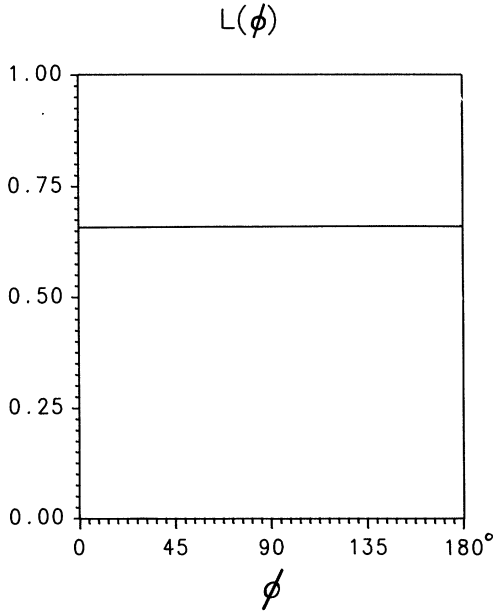


FIG. 7.  $L(\phi)$  factor in the folded azimuthal correlation function  $I(\phi) = L(\phi)[1 + \kappa'R(\phi)]$  for the  $\{\pi^-\pi^+\}$  spectrum.

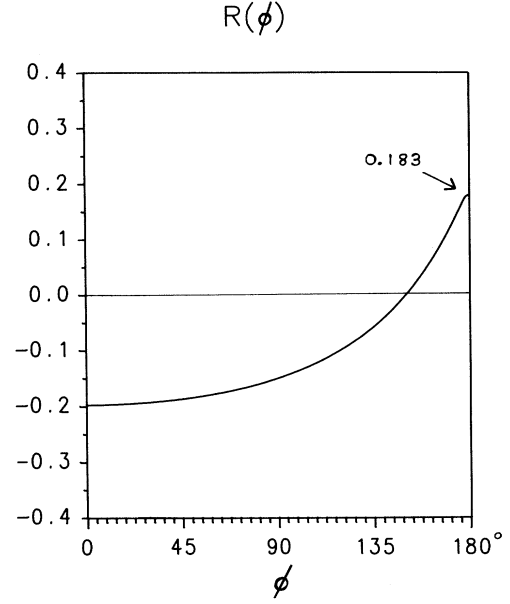


FIG. 8.  $R(\phi)$  term in the folded azimuthal correlation function for the  $\{\pi^-\pi^+\}$  spectrum.

integrate out  $\phi_e$ . The resulting distribution

$$I_>(\phi) = L(\phi)[1 + \kappa'R(\phi)]$$

is shown in Figs. 6 and 7. Events with  $\phi_e$  in the range  $-90^\circ - 0^\circ$  can be similarly integrated over  $\phi_e$  to obtain

$$I_<(\phi) = L(\phi)[1 - \kappa'R(\phi)]. \quad (2.12b)$$

We call  $I(\phi)$  the “folded azimuthal correlation function.” [Explicit expressions for  $L$  and  $R$  in Eqs. (2.12a) and (2.12b) are given by Eqs. (5.7) and (5.8) in Sec. V.]

In Table II are tabulated the ideal statistical errors<sup>20</sup> for measurement of  $\kappa'$  by the azimuthal correlation function  $I(\phi_e, \phi)$  and by the full beam-referenced  $\tau$  spin-correlation function  $I(\theta_e, \phi_e, E_1, E_2, \phi)$ , assuming  $10^7 Z^0$  events. The  $\{\pi^-\pi^+\}$  decay mode gives the smallest ideal statistical errors. For the folded azimuthal correlation function  $I(\phi)$ , we find a statistical error of  $\sigma(\kappa') = 0.109$ . On the other hand, if the polar angle  $\theta_e$  for the  $e^-$  beam is not integrated out (this angle is shown in Fig. 2), then the associated  $I(\theta_e, \phi_e, \phi)$  gives  $\sigma(\kappa') = 0.0798$ .

Also tabulated are the results of the other major two-body  $\tau$  decay channels assuming a pure  $V-A$  coupling for  $\tau^- \rightarrow h^- \nu$ . When  $h^-$  is not spin zero, a “hadron helicity parameter” [see Eq. (6.2)]

$$\mathcal{S}_h = \frac{m_\tau^2 - 2m_h^2}{m_\tau^2 + 2m_h^2} \quad (2.13)$$

appears in  $L$  and  $K'$ . In particular,  $K'$  is proportional to  $\mathcal{S}_A \mathcal{S}_B$  for the  $\{A^-, B^+\}$  spectrum, which suppresses the signature for  $\kappa'$ . Thus modes listed in later tables in this paper have been omitted from Table II if they gave a

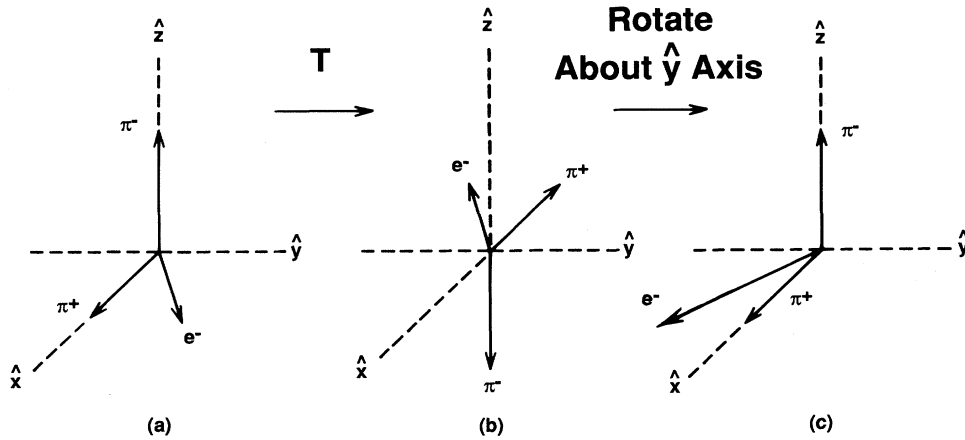


FIG. 9. Assuming a first-order Hermitian effective Hamiltonian, by time-reversal invariance and rotational invariance, decay (a) is equivalent to decay (c).

$\sigma(\kappa')$  greater than 1.

For the  $\{\pi^-\rho^+\}$  spectrum, the larger number of events almost compensates for the extra  $\mathcal{S}_\rho$  factor in  $K'$ . For it, for  $I(\phi)$  we find  $\sigma(k')=0.116$  and for  $I(\theta_e, \phi_e, \phi)$ ,  $\sigma(\kappa)=0.0871$ . We find the  $R$  figures for  $\{\pi^-\rho^+\}$  are as shown in Figs. 5 and 8 except

$$\begin{aligned}
 R_{\pi^-\rho^+} &\simeq \mathcal{S}_\rho R_{\pi^-\pi^+} \\
 &\simeq 0.457 R_{\pi^-\pi^+}, \tag{2.14a}
 \end{aligned}$$

and

$$L_{\pi^-\rho^+} \simeq L_{\pi^-\pi^+}. \tag{2.14b}$$

Clearly,  $L$  and  $R$  differ significantly in their dependence on  $\phi$ . With  $10^7 Z^0$  events, such a striking signature should enable a test to the few percent level for whether the violation of  $P$ , and of  $C$ , is indeed maximal in the  $Z^0 \rightarrow \tau^-\tau^+$  decay process.

Unlike for  $\tau$  spin-correlation functions  $I(E_1, E_2)$  and

TABLE II. Comparison of ideal statistical errors for  $\kappa'$  from measurements by the full beam-referenced  $\tau$  spin-correlation function  $I(\theta_e, \phi_e, E_1, E_2, \phi)$  with those from measurements by the simpler azimuthal correlation function  $I(\phi_e, \phi)$ . A nonzero value for  $\kappa'$  is the signature for other than maximal  $P$ , maximal  $C$  violation in  $Z^0 \rightarrow \tau^-\tau^+$  decay; that is,  $\kappa'=0$  at Born level in the standard model. Superscripts a and b denote the smallest and next smallest ideal statistical error for a single decay mode. Note that the ideal statistical errors are about the same for the  $\{\pi^-\pi^+\}$  and  $\{\pi^-\rho^+\}$  spectra.  $10^7 Z^0$  events have been assumed.

Sequential decay mode	Number of events	Comparison of ideal statistical errors	
		$I(\theta_e, \phi_e, E_1, E_2, \phi)$	$I(\phi_e, \phi)$
$\pi^-\pi^+$	3 861	0.0619 <sup>a</sup>	0.0970 <sup>a</sup>
$\pi^-K^+$	500	0.1707	0.2660
$\pi^-\rho^+$	16 087	0.0719 <sup>b</sup>	0.1044 <sup>b</sup>
$\pi^-K^+$	1 001	0.4029	0.5822
$K^-\pi^+$	1 043	0.2772	0.3949
$\rho^-\rho^+$	16 757	0.1492	0.2087
$\rho^-K^{*+}$	2 085	0.5822	0.8087
Sum of above modes	41 334	0.042	0.064 factor worse=1.50
Sum of $\pi^-\pi^+, \pi^-\rho^+$	19 948	0.047	0.071 factor worse=1.51

<sup>a</sup>Smallest.

<sup>b</sup>Next smallest.

$I(E_1, E_2, \phi)$  which, because of a factorization property<sup>10</sup> are similar to  $A_{LR}^{\mu^+\mu^-}$ , the radiative corrections needed for a high-precision measurements of  $I(\phi_e, \phi)$  or some other BRSC are more analogous to those for  $A_{FB}$ . Because of  $\theta_e$  and/or  $\phi_e$ , both the initial and final states are involved in the correlation. Note that  $I(\phi_e, \phi)$  is much less sensitive than  $A_{FB}$  to interference of initial- and final-state bremsstrahlung since in the signature region  $e^-$  is not in general parallel to  $\tau^-$ . The energy smearing and  $\gamma^* - Z^0$  interference effects will also be much less important for  $I(\phi_e, \phi)$  than for  $A_{FB}$  because there is already a  $\gamma^*$  effect in  $A_{FB}$ , whereas  $\gamma^*$  does not produce an odd  $\phi_e$  component in  $I(\phi_e, \phi)$  in the standard model.

Unlike the  $A_{FB}$ , additional one-loop electroweak corrections to the decays  $\tau^- \rightarrow h^- \nu$  can contribute here as may some higher-order QED corrections associated with the occurrence of a final decay sequence, instead of only an  $f\bar{f}$  final state, but again these corrections should be small ones. Most of the theoretical and experimental corrections to Figs. 4–8 and to the ideal statistical errors  $\sigma(\kappa')$  can best be investigated by  $\tau$ -pair Monte Carlo simulations.<sup>15</sup>

### B. Remarks

(i) From Eqs. (2.10) and (2.11), we see that if  $\kappa' \neq 0$ , then neglecting radiative and other corrections,

$$I(\phi_e, \phi)|_{\text{expt}} - I(\phi_e, \phi)|_{\text{SM}} = \text{const} \times \sin(2\phi_e) K'(\phi), \quad (2.15)$$

where  $K'(\phi)$  is given by Eq. (2.11b).

(ii) There is also a natural sensitivity check that can be used in the data analysis in the measurement of  $\kappa'$ . In the standard model there is a nonvanishing decay intensity parameter  $\kappa$ :

$$\kappa \equiv \frac{2}{\mathcal{N}} \text{Re}[T(+ -)T^*(- - +)] \\ \rightarrow (1 - r_\tau^2)M^2/\mathcal{N} = \frac{v^2 - a^2}{v^2 + a^2} = -0.987, \quad (2.16)$$

where  $\mathcal{N}$  is defined above in Eq. (2.7). The azimuthal correlation function  $I(\phi_e, \phi)$  is sensitive to  $\kappa$  (See the following, subsection.) The associated ideal statistical errors for measurement of  $\kappa$  are listed in Table III for the  $\{\pi^- \pi^+\}$  and  $\{\pi^- \rho^+\}$  spectra.

(iii) An aplanarity test of the  $e^-$  momentum versus the  $\pi_1^- \pi_2^+$  momenta plane is available here: From consideration of Fig. 5, one can define

$$A_{\text{aplanarity}} = \frac{N_{1,3} - N_{2,4}}{N_{1,3} + N_{2,4}}, \quad (2.17)$$

with

---

$N_{1,3}$  = total number of events with  $\phi_e$  in first plus third quadrant

$$\left[ 0 \leq \phi_e \leq \pi/2 \text{ or } -\frac{\pi}{2} \geq \phi_e \geq -\pi \right],$$

$N_{2,4}$  = total number of events with  $\phi_e$  in second plus fourth quadrant

$$\left[ \frac{\pi}{2} \leq \phi_e \leq \pi \text{ or } 0 \geq \phi_e \geq -\frac{\pi}{2} \right].$$

However, both Figs 5 and 8 with Eq. (2.11b) show that the integration over  $\phi$  reduces the sensitivity of  $A_{\text{aplanarity}}$  in measurement of  $\kappa'$ . This reduction can be avoided by a cut  $\phi < \sim 152^\circ$ , which removes some of the most back-to-back events. Due to limitations on angular resolution, this type of cut may be needed anyway.

(iv) The time-reversal argument associated with Fig. 9 applies to using  $I(\phi_e, \phi)$  for  $\tau$  leptonic decay modes, that is, for the  $\{l_1^- l_2^+\}$  and  $\{l_1^- h_2^+\}$  sequential decay channels. For three-body  $\tau$  decay modes, an effective  $\phi$  variable can be defined using Eqs. (3.15), (3.5), and (3.9a). Likewise, for  $e^-e^+$  collisions in the  $\Upsilon$  or  $J/\psi$  regions,

TABLE III. Comparison of ideal statistical errors for  $\kappa$  from measurements by  $I(\theta_e, \phi_e, E_1, E_2, \phi)$  with those from  $I(\phi_e, \phi)$ .

Sequential decay mode	Number of events	Comparison of ideal statistical errors $\sigma(\kappa)$	
		$I(\theta_e, \phi_e, E_1, E_2, \phi)$	$I(\phi_e, \phi)$
$\pi^- \pi^+$	3861	0.0478	0.0952
$\pi^- \rho^+$	16087	0.0700	0.1040
Sum of $\pi^- \pi^+, \pi^- \rho^+$	19948	0.0395	0.0702
			factor worse = 1.78

the  $\phi_e$  behavior of  $I(\phi_e, \phi)$  can be used to test for a complex phase in the  $\gamma^* \rightarrow \tau^- \tau^+$  coupling. If  $I(\phi_e, \phi)$  has an odd component when  $\phi_e \rightarrow \phi_e$ , then such a phase is present. [For these two generalizations, the associated explicit  $L(\phi_e, \phi)$  distribution in the standard model and the associated explicit  $\kappa'$  analyzing power distribution  $R(\phi_e, \phi) = K'(\phi_e, \phi) / L(\phi_e, \phi)$  has not yet been calculated.]

### C. Determination of $|\kappa'|$ from unitarity equality

The magnitude of  $\kappa'$ , we refer to it as  $|\kappa'|$ , can be determined alternatively by the "unitarity equality"

$$\kappa'^2 + \kappa^2 = (1 - \delta)^2 + \alpha^2, \quad (2.18)$$

where the additional  $Z^0$  decay intensity parameters are

$$(1 - \delta) = \frac{1}{\mathcal{N}} [ |T(+ -)|^2 + |T(- +)|^2 ] \rightarrow 1, \quad (2.19a)$$

$$\alpha = \frac{1}{\mathcal{N}} [ |T(+ -)|^2 - |T(- +)|^2 ] \rightarrow -\frac{2r_\tau M^2}{\mathcal{N}} = -\frac{2av}{v^2 + a^2} = -0.159, \quad (2.19b)$$

and  $\kappa'$  and  $\kappa$  are given above by Eqs. (2.6) and (2.16). Note that the  $\delta$  parameter is

$$\delta = \frac{1}{\mathcal{N}} [ |T(++)|^2 + |T(--)|^2 ] \rightarrow 0. \quad (2.20)$$

Therefore, Eq. (2.18) can be used to determine  $\kappa'$  if the three intensity parameters  $\delta$ ,  $\alpha$ , and  $\kappa$  are measured. These  $(\delta, \alpha, \kappa)$  are, in principle, independent parameters and can all be measured independently from  $I(\theta_e, \phi_e, E_1, E_2, \phi)$ .

Since  $\delta$  is zero in the standard-model, Born-level, limit, we list in Table IV associated ideal statistical errors for the  $\{\pi^- \pi^+\}$  and  $\{\pi^- \rho^+\}$  spectra when  $\alpha$  and  $\kappa$  are measured from  $I(\theta_e, \phi_e, E_1, E_2, \phi)$ . Note that since the magnitude of  $\kappa'$  is at present unknown, the error for  $|\kappa'| \sigma(\kappa')$  is listed.

Note also that while  $\delta$  and  $\alpha$  can be measured by the simpler distributions such as the energy correlation  $I(E_1, E_2)$ , to be sensitive to  $\kappa$  requires inclusion of the  $\phi_e$

TABLE IV. ideal statistical errors associated with the measurement of the magnitude of  $\kappa'$  by use of the unitarity equality of Eq. (2.18). The errors for  $\kappa$  and  $\alpha$  are from measurements by  $I(\theta_e, \phi_e, E_1, E_2, \phi)$ . See text for remarks about how simpler angular distributions can be used to measure  $\alpha$  and  $\kappa$ .

Sequential decay mode	Number of events	$ \kappa'  \sigma(\kappa')$	$ \alpha  \sigma(\alpha)$	$ \kappa  \sigma(\kappa)$
$\pi^- \pi^+$	3861	0.0473	0.003 45	0.0471
$\pi^- \rho^+$	16 087	0.0692	0.002 02	0.0691
Sum of $\pi^- \pi^+, \pi^- \rho^+$	19 948	0.0390		

dependence. The errors for  $\kappa$  from  $I(\phi_e, \phi)$  were listed in Table III. In  $I(\phi_e, \phi)$  the  $\kappa$ -dependent term has a pure  $\cos(2\phi_e)$  dependence on  $\phi_e$ . But there is also a  $\cos(2\phi_e)$  dependence, as well as constant and  $\cos(\phi_e)$  dependencies, in the  $(1 - \delta)$  and  $\alpha$  terms. [See Eq. (5.2a) in Sec. V below.]

Finally, we stress that measurement of  $\delta$ ,  $\alpha$ ,  $\kappa$ , and  $\kappa'$  will completely determine the fundamental helicity amplitudes  $T(-+)$  and  $T(+-)$ .

### III. KINEMATICS

We discuss the kinematics of the production-decay sequence

$$e^- e^+ \rightarrow Z^0 \rightarrow \tau_1^- \tau_2^+ \rightarrow (\pi_1^- \nu) (\pi_2^+ \bar{\nu}). \quad (3.1)$$

The  $e^- e^+ \rightarrow Z^0 \rightarrow \tau_1^- \tau_2^+$  part is shown in Fig. 10 for the  $Z^0$  rest frame. The  $\tau_1^-$  and  $\tau_2^+$  momenta are, of course, back to back. We assume that the  $\nu$  and  $\bar{\nu}$  momenta are not measured, and so the observed part of the production-decay sequence is as shown in Fig. 11. The polar angle  $\theta_e$  describes the distribution of the final  $\pi_1^-$  relative to the initial  $e^-$  beam direction.

In Fig. 12 these two figures have been overlaid to exhibit the angles  $\theta_{1,2}$  between each pion's momentum and its associated  $\tau$ 's momentum direction. The angle  $\theta_1$  and the  $\pi_1^-$  energy  $E_1$  are, in fact, not independent. To see this, first note that  $\cos \theta_1$  is known since with  $p_1$  the magnitude of the  $\pi_1^-$  momentum

$$2\tilde{P} p_1 \cos \theta_1 = 2\tilde{P}_0 E_1 - m^2 - \mu_1^2, \quad (3.2)$$

where  $\tilde{P}_0 = M/2$ ,  $\tilde{P}^2 = \tilde{P}_0^2 - m^2$ , with  $M =$  the  $Z^0$  mass,  $m =$  the  $\tau$  mass, and  $\mu_1 =$  the  $\pi_1^-$  mass. By squaring, Eq. (3.2) easily yields the kinematic limits to  $E_1$ . See Eq. (3.6c) below. From the  $\gamma$  and  $\beta$  for the relativistic boost to the  $\tau_1^-$  rest frame [ $\gamma = M/(2m)$ ] the helicity polar angle  $\theta_1'$  (see Fig. 3) is determined by

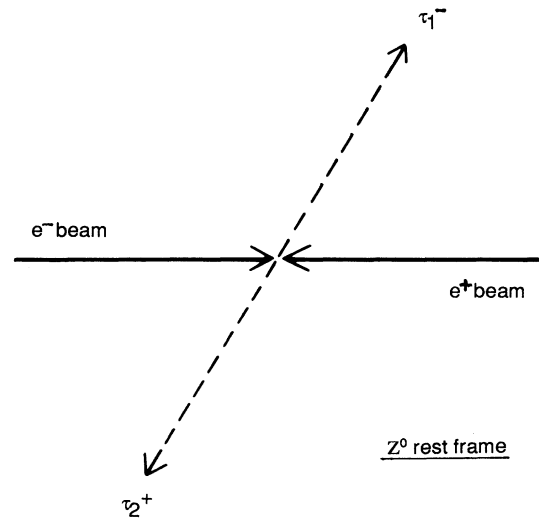


FIG. 10.  $e^- e^+ \rightarrow Z^0 \rightarrow \tau_1^- \tau_2^+$  part of the production-decay sequence  $e^- e^+ \rightarrow Z^0 \rightarrow \tau_1^- \tau_2^+ \rightarrow (\pi_1^- \nu) (\pi_2^+ \bar{\nu})$ . The  $\tau_1^-$  and  $\tau_2^+$  momenta are back to back in the  $Z^0$  rest frame.



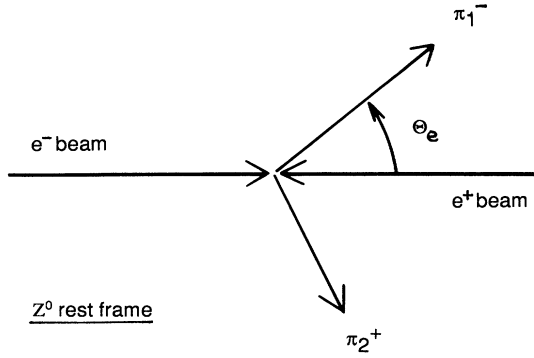


FIG. 11. Observable part of the production-decay sequence  $e^-e^+ \rightarrow Z^0 \rightarrow \tau_1^- \tau_2^+ \rightarrow (\pi_1^- \nu)(\pi_2^+ \bar{\nu})$ . The polar angle  $\theta_e$  describes the distribution of the final  $\pi_1^-$  relative to the  $e^-$  beam direction, in the  $Z^0$  rest frame. The  $\pi_1^-$  and  $\pi_2^+$  do not, in general, both lie in the beam plane.

$$p_1^\tau \cos \theta_1^\tau = \gamma(p_1 \cos \theta_1 - \beta E_1) \quad (3.3)$$

since  $0 \leq \theta_1^\tau \leq \pi$ . In Eq. (3.3) the magnitude of the  $\pi_1^-$  momentum in the  $\tau_1^-$  rest frame is, of course,

$$p_1^\tau = \frac{m^2 - \mu_1^2}{2m}, \quad E_1^\tau = [\mu_1^2 + (p_1^\tau)^2]^{1/2}. \quad (3.4)$$

This then yields  $\theta_1$  since

$$p_1^\tau \sin \theta_1^\tau = p_1 \sin \theta_1.$$

Throughout this paper the  $\tau$  superscripts denote the respective  $\tau$  rest-frame variables and the variables free of superscripts are for the  $Z^0$  rest frame. The angles  $\phi, \phi_1, \phi_2$

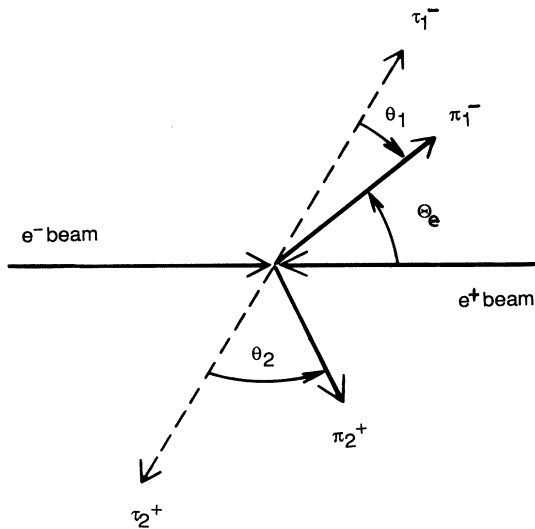


FIG. 12. Figures 10 and 11 overlaid. The angle  $\theta_1$  between the  $\pi_1^-$  and  $\tau_1^-$  directions is equivalent to the  $\pi_1^-$  energy  $E_1$  [see Eq. (3.2)]. Similarly, the angle  $\theta_2$  and the  $\pi_2^+$  energy  $E_2$  are equivalent variables [see Eq. (3.8)]. Since the  $\tau_1^-$  and  $\tau_2^+$  momenta are back to back, the angles  $\theta_1$  and  $\theta_2$  determine the  $\tau_1^-$  momentum direction, up to a twofold ambiguity, as shown in Fig. 13.

are Lorentz invariant under boosts connecting the three frames.

In summary

$$\theta_1^\tau = \arccos \left[ \frac{-M(m^2 + \mu_1^2) + 4E_1 m^2}{(m^2 - \mu_1^2)\sqrt{M^2 - 4m^2}} \right], \quad 0 \leq \theta_1^\tau \leq \pi. \quad (3.5a)$$

Note that

$$\cos \theta_1^\tau = [2(E_1/E_1^{\max}) - 1][1 + O((m/M)^2)], \quad (3.5b)$$

where, from Eq. (3.2),

$$E_1^{\max, \min} = \frac{M(m^2 + \mu_1^2)}{4m^2} \pm \frac{M(m^2 - \mu_1^2)}{4m^2} \left[ 1 - \frac{4m^2}{M^2} \right]^{1/2}. \quad (3.5c)$$

Then the angle  $\theta_1$  is determined uniquely from  $\cos \theta_1$  and  $\sin \theta_1$  of

$$p_1 \cos \theta_1 = \gamma(p_1^\tau \cos \theta_1^\tau + \beta E_1^\tau), \quad (3.6a)$$

$$p_1 \sin \theta_1 = p_1^\tau \sin \theta_1^\tau. \quad (3.6b)$$

A check is

$$E_1 = \gamma(E_1^\tau + \beta p_1^\tau \cos \theta_1^\tau). \quad (3.7)$$

By the obvious symmetrical relabeling, the analogous formulas are obtained for the  $\pi_2^+$ : Again,  $\cos \theta_2$  is known from  $E_2$  since

$$2\tilde{P}p_2 \cos \theta_2 = 2\tilde{P}_0 E_2 - m^2 - \mu_2^2 \quad (3.8)$$

is the analog of Eq. (3.2). In summary,

$$\theta_2^\tau = \arccos \left[ \frac{-M(m^2 + \mu_2^2) + 4E_2 m^2}{(m^2 - \mu_2^2)\sqrt{M^2 - 4m^2}} \right], \quad 0 \leq \theta_2^\tau \leq \pi, \quad (3.9a)$$

where  $E_2$  is the  $\pi_2^+$  energy in the  $Z^0$  rest frame and  $\mu_2$  is the  $\pi_2^+$  mass. Also,

$$\cos \theta_2^\tau = [2(E_2/E_2^{\max}) - 1][1 + O((m/M)^2)], \quad (3.9b)$$

and

$$E_2^{\max, \min} = \frac{M(m^2 + \mu_2^2)}{4m^2} \pm \frac{M(m^2 - \mu_2^2)}{4m^2} \left[ 1 - \frac{4m^2}{M^2} \right]^{1/2}. \quad (3.9c)$$

The angle  $\theta_2$  is determined uniquely from  $\cos \theta_2$  and  $\sin \theta_2$  of

$$p_2 \cos \theta_2 = \gamma(p_2^\tau \cos \theta_2^\tau + \beta E_2^\tau), \quad (3.10a)$$

$$p_2 \sin \theta_2 = p_2^\tau \sin \theta_2^\tau, \quad (3.10b)$$

where  $p_2$  is the magnitude of the  $\pi_2^+$  momentum in the  $Z^0$  rest frame. Its magnitude in the  $\tau_2^+$  rest frame is

$$p_2^\tau = \frac{m^2 - \mu_2^2}{2m},$$

$$E_2^\tau = [\mu_2^2 + (p_2^\tau)^2]^{1/2}. \quad (3.11)$$

A check is

$$E_2 = \gamma(E_2^\tau + \beta p_2^\tau \cos\theta_2^\tau). \quad (3.12)$$

#### A. *A- or B-axis ambiguity in the $\tau_1^-$ momentum direction*

Up to an ambiguity as to whether to use an *A* or a *B* axis, the direction of the  $\tau_1^-$  momentum can be determined<sup>21</sup> using some of the formulas listed above, as we now explain.

For a given  $\{\pi_1^-, \pi_2^+\}$  event corresponding to the production-decay sequence of Eq. (3.1), we know the angle  $\theta_1$  from Eqs. (3.6a) and (3.6b), and similarly the angle  $\theta_2$  from Eqs. (3.10a) and (3.10b). So, as illustrated in Fig. 13, on the unit sphere a circle of angle  $\theta_1$  about the  $\pi_1^-$  momentum direction can be inscribed. Then another circle of angle  $(\pi - \theta_2)$  about the  $\pi_2^+$  momentum direction can also be inscribed. In general, these circles will intersect at two points. One of these points is the *A* axis and the other is the *B* axis. The  $\tau_1^-$  momentum direction lies along one of these two axes. (Experimentally, the correct axis would be known if either of the missing  $\nu$  and  $\bar{\nu}$  momentum in the  $\tau$  decays were measured.)

Note that

$$\phi_A + \phi_B = 2\pi, \quad (3.13a)$$

where  $\phi_A$  and  $\phi_B$  are defined in Fig. 13. Thus

$$\cos\phi_A = \cos\phi_B = \cos\phi, \quad (3.13b)$$

but

$$\sin\phi_A = -\sin\phi_B. \quad (3.13c)$$

This  $\phi$  angle is, of course, the very important<sup>18,21</sup> angle between the  $\tau_1^-$  and  $\tau_2^+$  decay planes.

The upshot of this twofold ambiguity in the  $\tau_1^-$

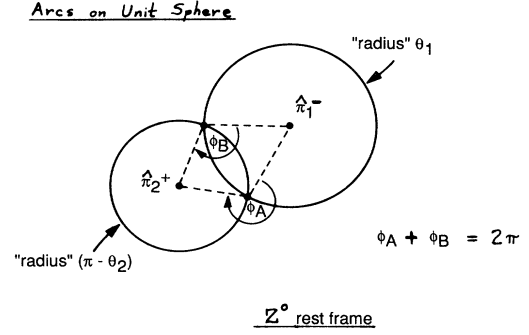


FIG. 13. Illustration on the unit sphere of the twofold *A- or B-axis ambiguity* as to the  $\tau_1^-$  momentum direction in the  $Z^0$  rest frame. Note that  $\phi_A + \phi_B = 360^\circ$ , and so  $\cos\phi_A = \cos\phi_B$ , but  $\sin\phi_A = -\sin\phi_B$ . This  $\phi$  angle is, of course, simply the angle between the  $\tau_1^-$  and  $\tau_2^+$  decay planes. Therefore,  $\cos\phi$  is measurable [see Eq. (3.15)], but the sign of  $\sin\phi$  is not, because of the missing  $\nu$  and  $\bar{\nu}$  momenta.

momentum direction, therefore, is simply that  $\cos\phi$  is measurable for each  $\{\pi_1^-, \pi_2^+\}$  event, but that  $\sin\phi$  is not because of the missing  $\nu$  and  $\bar{\nu}$  momenta.

In the analysis of elementary-particle reactions, one is accustomed to having to investigate out the kinematic variables of the missing neutral particles, consistent with the other kinematic constraints. Here, for the production-decay sequence of Eq. (3.1), instead of an integration, there is a simple summation over the two possible signs of  $\sin\phi$ .

Finally, since  $\theta_1$  and  $\theta_2$  are known, the  $\cos\phi$  can be expressed explicitly in terms of the cosine of the opening angle  $\psi$  between the  $\pi_1^-$  and  $\pi_2^+$  momenta in the  $Z^0$  rest frame. (See again Fig. 2.) The quantity  $\cos\phi$  can be obtained from

$$\cos\psi = -\cos\theta_1\cos\theta_2 + \sin\theta_1\sin\theta_2\cos\phi. \quad (3.14)$$

Equivalently, since  $\theta_1^\tau$  and  $\theta_2^\tau$  are known from the summary equations (3.5) and (3.9), we find that  $\cos\phi$  is given explicitly by

$$\sin\theta_1^\tau\sin\theta_2^\tau\cos\phi = \frac{4m^2}{(m^2 - \mu_1^2)(m^2 - \mu_2^2)} \left[ p_1 p_2 \cos\psi + \frac{(ME_1 - m^2 - \mu_1^2)(ME_2 - m^2 - \mu_2^2)}{M^2 - 4m^2} \right]. \quad (3.15)$$

#### B. Summary and illustration

In thinking about the sequential decay

$$Z^0 \rightarrow \begin{array}{l} \tau^- \quad \tau^+ \\ \quad \quad \quad \searrow \quad \swarrow \\ \quad \quad \quad \pi_2^+ \bar{\nu} \\ \quad \quad \quad \swarrow \quad \searrow \\ \quad \quad \quad \pi_1^- \nu \end{array} \quad (3.16)$$

and the interrelation among the three rest frames, Fig. 14 is often useful. See its caption.

#### C. $\phi$ -bypass procedure for event labeling

Once recognized and understood, it is clear that this *A- and B-axis ambiguity* does not complicate event analysis. When the  $\nu$  and  $\bar{\nu}$  momenta are not measured by the detector, we can simply choose  $\sin\phi$  to be positive. That is, we choose  $\phi$  to lie in the range  $0 \leq \phi \leq \pi$ . So, from  $E_1$ ,  $E_2$ , and  $\psi$  for each event, we can easily use Eqs. (3.14) with (3.5) and (3.9) to derive the  $\phi$  label for that event. We call this the “ $\phi$ -bypass” convention or procedure. With this bypass, we have labeled each event in  $\phi$  and can consider it in either the  $Z^0$  rest frame, the  $\tau_1^-$

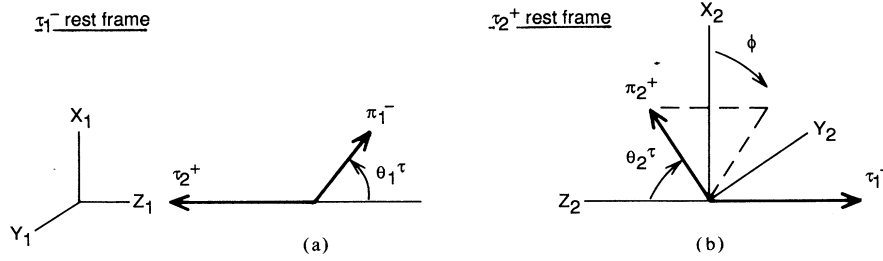


FIG. 14. Summary illustration showing the three angles  $\theta_1^-$ ,  $\theta_2^+$ , and  $\phi$  describing the sequential decay  $Z^0 \rightarrow \tau_1^- \tau_2^+$  with  $\tau_1^- \rightarrow \pi_1^- \nu$  and  $\tau_2^+ \rightarrow \pi_2^+ \bar{\nu}$ . In (a) the missing  $\nu$  momentum, not shown, is back to back with the  $\pi_1^-$ . In (b) the missing  $\bar{\nu}$  momentum, also not shown, is back to back with the  $\pi_2^+$ . From (a) a boost along the negative  $z_1$  axis transforms the kinematics from the  $\tau_1^-$  rest frame to the  $Z^0$  rest frame and, if boosted further, to the  $\tau_2^+$  rest frame shown in (b).

rest frame, and/or the  $\tau_2^+$  rest frame. (But this is only for convenience in event labeling; see next paragraph.)

If one wanted to experimentally search<sup>22,23</sup> for physical  $\nu_\tau$ - and  $\bar{\nu}_\tau$ -induced reactions, one could use  $\cos\phi$ 's value. Then one would first choose  $0 \leq \phi \leq \pi$  and look in the  $\nu_\tau$  direction [see Fig. 14(a)] and  $\bar{\nu}_\tau$  direction [see Fig. 14(b)] for possible candidate  $\nu_\tau$  (or  $\bar{\nu}_\tau$ ) reactions in the detector. Then one must also choose  $\pi < \phi \leq 2\pi$  and perform the same search. Of course, the final-state kinematics here are not special to  $e^-e^+$  collisions at the  $Z^0$  and so the  $\nu_\tau$  and  $\bar{\nu}_\tau$  directions are also known, up to this twofold ambiguity for  $\tau^-\tau^+$  production at other center-of-mass energies. However, even at the proposed  $\tau$ /charm factory, the  $\nu_\tau$  and  $\bar{\nu}_\tau$  fluxes are much too meager and nothing would be found by such a search unless the  $\nu_\tau$  or  $\bar{\nu}_\tau$  were to have nonweak interactions with the target. Constraints from  $\tau$  partial decay widths and the  $Z^0$  invisible width make this option very unlikely for  $\nu_\tau$  or  $\bar{\nu}_\tau$  incident on ordinary nuclei.

#### IV. DERIVATION OF THE BEAM-REFERENCED $\tau$ SPIN-CORRELATION FUNCTION AT THE $Z^0$

In this section we derive the BRSC function for the production-decay sequence

$$e^-e^+ \rightarrow Z^0 \rightarrow \tau_1^- \tau_2^+ \rightarrow (\pi_1^- \nu) (\pi_2^+ \bar{\nu}). \quad (4.1)$$

It will be generalized to other  $\tau$  two-body decay modes in Sec. VI. Then the chirality parameter  $\xi_h$  for describing the chirality of the  $\tau^- \rightarrow h^- \nu$  coupling will also be included, as will the hadron helicity parameter  $\mathcal{S}_h$ . In the present section we assume the standard  $V-A$  coupling, i.e.,  $\xi = 1$ , for  $\tau^- \rightarrow \pi^- \nu$  decay.

##### A. $\tau_1^- \tau_2^+$ production density matrix at the $Z^0$

The matrix element for the decay of the  $Z^0$  into  $\tau_1^- \tau_2^+$  is defined by

$$\langle \Theta_\tau, \Phi_\tau, \lambda_1, \lambda_2 | JM \rangle = D_{M\lambda}^{J*}(\Phi_\tau, \Theta_\tau, -\Phi_\tau) T(\lambda_1, \lambda_2), \quad (4.2)$$

where  $\lambda_1, \lambda_2$  denote, respectively, the helicities of the  $\tau_1^-$  and  $\tau_2^+$  and  $\lambda = \lambda_1 - \lambda_2$ . Since  $Z^0$  has spin zero,  $J=1$ . The angle  $s$  is defined in the  $Z^0$  rest frame in the usual way; see Fig. 14.

The matrix appearing in Eq. (4.2) is related to the  $d$  functions by

$$D_{M\lambda}^J(\phi, \theta, -\phi) = e^{i(\lambda-M)\phi} d_{M\lambda}^J(\theta).$$

The phase convention of Rose<sup>24</sup> is to be used for the  $d$

functions, for this is part of the Jacob-Wick phase convention.<sup>16</sup>

When  $Z^0 \rightarrow \tau_1^- \tau_2^+$  is invariant under  $CP$ , since  $\tau_1^-$  and  $\tau_2^+$  are a particle-antiparticle pair,

$$T(\lambda_1, \lambda_2) = \gamma_{CP} T(-\lambda_2, -\lambda_1), \quad (4.3)$$

where  $\gamma_{CP}$  is the  $CP$  quantum number of the  $Z^0$ . Similarly, if this decay were  $P$  invariant,

$$T(\lambda_1, \lambda_2) = \eta_P (-)^J T(-\lambda_1, -\lambda_2), \quad (4.4)$$

where  $\eta_P$  is the parity quantum number of the  $Z^0$  system ( $\eta_P = -1$  in the SM). If this decay were  $C$  invariant,

$$T(\lambda_1, \lambda_2) = C_n (-)^J T(\lambda_2, \lambda_1), \quad (4.5)$$

where  $C_n$  is the charge-conjugation eigenvalue of the  $Z^0$  ( $C_n = -1$  in the SM).

Likewise, the matrix element for the formation of the  $Z^0$  in the center-of-mass frame from an  $e^-e^+$  collision is defined by

$$\langle JM | \Theta_B, \Phi_B, s_1 s_2 | \rangle = D_{Ms}^J(\Phi_B, \Theta_B, -\Phi_B) \tilde{T}(s_1, s_2), \quad (4.6)$$

where  $\Theta_B$  and  $\Phi_B$  specify the  $e^-$  (beam) momentum. (Simply relabel  $\tau \rightarrow e$  in Fig. 14 with  $\Theta_\tau, \Phi_\tau \rightarrow \Theta_B, \Phi_B$ . The  $z$  axis, of course, is still the  $Z^0$  polarization axis). In Eq. (4.6)  $s_1$  and  $s_2$  denote, respectively, the helicities of  $e_1^-$  and  $e_2^+$  with  $s = s_1 - s_2$  and  $J=1$ .

If  $\tau$ -electron universality and time-reversal invariance hold, the amplitudes in Eqs. (4.2) and (4.6) are, of course, related:

$$\tilde{T}(\lambda_1, \lambda_2) = T(\lambda_1, \lambda_2). \quad (4.7)$$

In terms of these two amplitudes  $T(\lambda_1, \lambda_2)$  and  $\tilde{T}(s_1, s_2)$ , the amplitude for  $e^-e^+ \rightarrow \tau^- \tau^+$  scattering at the  $Z^0$  is

$$A_{s_1 s_2; \lambda_1 \lambda_2} = \sum_M D_{M\lambda}^{1*}(\Phi_\tau, \Theta_\tau, -\Phi_\tau) \times \frac{T(\lambda_1, \lambda_2) \tilde{T}(s_1, s_2)}{D_Z} D_{Ms}^1(\Phi_B, \Theta_B, -\Phi_B) \quad (4.8)$$

$$= \frac{T(\lambda_1, \lambda_2) \tilde{T}(s_1, s_2)}{D_Z} D_{\lambda s}^1(\Phi_B, \Theta_B, -\Phi_B), \quad (4.9)$$

where  $D_2 = s_Z - M^2 + iM\Gamma_Z$ . The simpler expression of Eq. (4.9) follows when the final  $\tau^-$  direction is chosen to

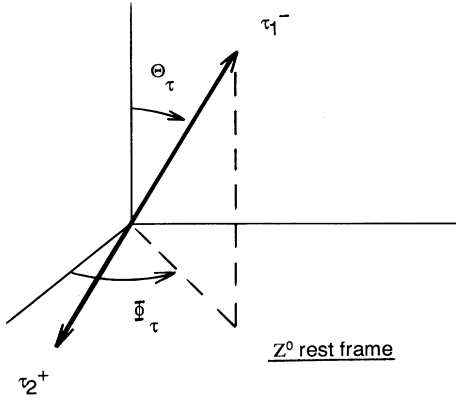


FIG. 15. Usual angles in the helicity formalism for describing the  $\tau_1^- \tau_2^+$  distribution in the  $Z^0$  rest frame. The  $z$  axis is the  $Z^0$ 's polarization axis.

coincide with the  $z$  axis of  $Z^0$  polarization (see Fig. 15), so that

$$D_{M\lambda}^{1*}(\Phi_\tau, 0, -\Phi_\tau) = e^{-i(\lambda-M)\Phi_\tau} d_{M\lambda}^1(0) = \delta_{M\lambda}. \quad (4.10)$$

Note that, in Eq. (4.9),

$$D_{\lambda s}^1(\Phi_B, \Theta_B, -\Phi_B) = e^{i(s-\lambda)\Phi_B} d_{\lambda s}^1(\Theta_B). \quad (4.11)$$

Thus, for initially unpolarized particles in the  $e^-e^+$  collision, we find the  $\tau_1^- \tau_2^+$  production density matrix

$$\rho_{\lambda_1 \lambda_2; \lambda'_1 \lambda'_2}^{\text{prod}} = \frac{T(\lambda_1, \lambda_2) T^*(\lambda'_1, \lambda'_2)}{|D_Z|^2} e^{i(\lambda' - \lambda)\Phi_B} \times \left[ \frac{1}{4} \sum_{s_1, s_2} |\tilde{T}(s_1, s_2)|^2 d_{\lambda s}^1(\Theta_B) d_{\lambda' s}^1(\Theta_B) \right], \quad (4.12)$$

where  $\lambda = \lambda_1 - \lambda_2$ ,  $\lambda' = \lambda'_1 - \lambda'_2$ , and  $s = s_1 - s_2$ .

### B. Derivation of the BRSC function at the $Z^0$

In the standard model, the decay matrix element for  $\tau_1^- \rightarrow \pi_1^- \nu$  decay is given simply by

$$\langle \theta_1^\tau, \phi_1, 0, -\frac{1}{2} | \frac{1}{2}, \lambda_2 \rangle = C D_{\lambda_1, 1/2}^{1/2*}(\phi_1, \theta_1^\tau, -\phi_1), \quad (4.13)$$

where  $C$  is a constant, irrelevant to this derivation. The angles are defined as usual in the helicity formalism; again see Fig. 2. Similarly, for  $\tau_2^+ \rightarrow \pi_2^+ \bar{\nu}$ ,

$$\langle \theta_2^\tau, \phi_2, 0, \frac{1}{2} | \frac{1}{2}, \lambda_2 \rangle = C' D_{\lambda_2, -1/2}^{1/2*}(\phi_2, \theta_2^\tau, -\phi_2). \quad (4.14)$$

The associated  $\tau$  decay density matrices are

$$\rho_{\lambda_1 \lambda_2; \lambda'_1 \lambda'_2}^{\text{prod}} \rightarrow \delta_{\lambda_2, -\lambda_1} \delta_{\lambda'_2, -\lambda'_1} \frac{T(\lambda_1, -\lambda_1) T^*(\lambda'_1, -\lambda'_1)}{|D_Z|^2} \times e^{i2(\lambda'_1 - \lambda_1)\Phi_B} \frac{1}{4} [|\tilde{T}(+-)|^2 d_{\lambda_1}^1(\Theta_B) d_{\lambda'_1}^1(\Theta_B) + |\tilde{T}(-+)|^2 d_{\lambda_1, -1}^1(\Theta_B) d_{\lambda'_1, -1}^1(\Theta_B)], \quad (4.18)$$

$$\rho_{\lambda_1 \lambda'_1}(\tau_1^- \rightarrow \pi_1^- \nu) = D_{\lambda_1, 1/2}^{1/2*}(\phi_1, \theta_1^\tau, -\phi_1) \times D_{\lambda'_1, 1/2}^{1/2}(\phi_1, \theta_1^\tau, -\phi_1), \quad (4.15a)$$

and

$$\rho_{\lambda_2 \lambda'_2}(\tau_2^+ \rightarrow \pi_2^+ \bar{\nu}) = D_{\lambda_2, -1/2}^{1/2*}(\phi_2, \theta_2^\tau, -\phi_2) \times D_{\lambda'_2, -1/2}^{1/2}(\phi_2, \theta_2^\tau, -\phi_2), \quad (4.15b)$$

where the two irrelevant constants  $C$  and  $C'$  have been omitted.<sup>19</sup>

Thus, associated with the production-decay sequence

$$e^- e^+ \rightarrow Z^0 \rightarrow \tau_1^- \tau_2^+ \rightarrow (\pi_1^- \nu)(\pi_2^+ \bar{\nu}),$$

the general angular distribution is

$$I(\Theta_B, \Phi_B, \theta_1^\tau, \phi_1, \theta_2^\tau, \phi_2) = \sum_{\substack{\lambda_1 \lambda_1 \\ \lambda'_1 \lambda'_2}} \rho_{\lambda_1 \lambda_2; \lambda'_1 \lambda'_2}^{\text{prod}}(e_1^- e_2^+ \rightarrow \tau_1^- \tau_2^+) \times \rho_{\lambda_1 \lambda'_1}(\tau_1^- \rightarrow \pi_1^- \nu) \rho_{\lambda_2 \lambda'_2}(\tau_2^+ \rightarrow \pi_2^+ \bar{\nu}), \quad (4.16)$$

where the three density matrices are given, respectively, by Eqs. (4.12), (4.15a), and (4.15b). With Eq. (4.16) there is an associated differential counting rate

$$dN = I(\Theta_B, \Phi_B, \theta_1^\tau, \phi_1, \theta_2^\tau, \phi_2) \times d(\cos\Theta_B) d\Phi_B d(\cos\theta_1^\tau) d\phi_1 d(\cos\theta_2^\tau) d\phi_2, \quad (4.17)$$

where, for full phase space, the cosine of each polar angle ranges from  $-1$  to  $1$ , and each azimuthal angle ranges from  $0$  to  $2\pi$ .

In the precision range of current interest at  $Z^0$  energies, some corrections due to finite  $e$  and  $\tau$  masses are negligible or of higher order. First, the effect in Eq. (4.16) from  $(m_e/M) \neq 0$  (i.e., from the nonzero electron mass) in the  $\tau_1^- \tau_2^+$  production density matrix is negligible.

Second, it is convenient to calculate separately the contribution quadratic in  $T(+ -)$  and/or  $T(- +)$ . This contribution survives in the  $m/M \rightarrow 0$  limit, where  $m = \tau$  mass and  $M = Z^0$  mass, and so we call it the order- $(1)$  contribution. The contributions linear and quadratic in  $T(++)$  and/or  $T(--)$  vanish, respectively, as  $(m/M)$  and  $(m/M)^2$  in the standard model. The analogous BRSC, which includes them, can be straightforwardly calculated. We refer to them, respectively, as the  $O(m/M)$  and  $O((m/M)^2)$  contributions. Note that in the present paper, except for not including these  $T(++)$  and  $T(--)$  contributions, we do not drop  $m/M$  or  $\mu/m$  effects in the analytic formulas.

So, ordering our calculation this way, we have

where  $\lambda = 2\lambda_1$  and  $\lambda' = 2\lambda'_1$ . After using the two Kronecker  $\delta$ 's from Eq. (4.18), the angular distribution of Eq. (4.16) has only four different terms quadratic in the  $Z^0 \rightarrow \tau_1^- \tau_2^+$  amplitudes,  $T(+ -)$  and  $T(- +)$ .

Each term can depend on

$$\phi = \phi_1 + \phi_2, \tag{4.19a}$$

the angle between the two  $\tau$  decay planes, and on the angular difference

$$\Phi_B - \phi_1. \tag{4.19b}$$

The angle  $\phi_1$  can therefore be integrated out.

Explicitly, the four terms are as follows. For  $\lambda_1 = \lambda'_1 = \frac{1}{2}$ ,

$$|T(+, -)|^2 \cos^2(\theta_1^\tau/2) \cos^2(\theta_2^\tau/2) [|\tilde{T}(+ -)|^2 \cos^4(\Theta_B/2) + |\tilde{T}(- +)|^2 \sin^4(\Theta_B/2)]. \tag{4.20a}$$

For  $\lambda_1 = \lambda'_1 = -\frac{1}{2}$ .

$$|T(-, +)|^2 \sin^2(\theta_1^\tau/2) \sin^2(\theta_2^\tau/2) [|\tilde{T}(+ -)|^2 \sin^4(\Theta_B/2) + |\tilde{T}(- +)|^2 \cos^4(\Theta_B/2)]. \tag{4.20b}$$

For  $\lambda_1 = -\lambda'_1 = \frac{1}{2}$ ,

$$T(+, -) T^*(-, +) e^{-i2(\Phi_B - \phi_1)} e^{-i\phi} \cos(\theta_1^\tau/2) \sin(\theta_2^\tau/2) \times [-\cos(\theta_2^\tau/2) \sin(\theta_2^\tau/2)] [|\tilde{T}(+ -)|^2 + |\tilde{T}(- +)|^2] \cos^2(\Theta_B/2) \sin^2(\Theta_B/2). \tag{4.20c}$$

For  $\lambda_1 = -\lambda'_1 = -\frac{1}{2}$ ,

$$T(-, +) T^*(+, -) e^{i2(\Phi_B - \phi_1)} e^{i\phi} \sin(\theta_1^\tau/2) \cos(\theta_2^\tau/2) \times [-\sin(\theta_2^\tau/2) \cos(\theta_2^\tau/2)] [|\tilde{T}(+ -)|^2 + |\tilde{T}(- +)|^2] \cos^2(\Theta_B/2) \sin^2(\Theta_B/2). \tag{4.20d}$$

### C. Structure of full $I(\dots)$ of Eq. (4.16)

From Eqs. (4.20a)–(4.20d), one can see that, in the helicity formalism, the full production-decay distribution has the form

$$I(\dots) = \sum \mathcal{P}(\dots) \mathcal{A}(\theta_1^\tau, \theta_2^\tau), \tag{4.21}$$

where

$$(\dots) = (\Theta_B, \Phi_B - \phi_1, \theta_1^\tau, \theta_2^\tau, \phi). \tag{4.22}$$

We refer to the  $\mathcal{P}(\dots)$  as  $Z^0$  production coefficients at the  $Z^0$  and the  $\mathcal{A}(\theta_1^\tau, \theta_2^\tau)$  as  $Z^0$  decay analyzer coefficients. If the  $\nu$  and  $\bar{\nu}$  momenta directions were measured, then all the angles in Eq. (4.22) would be measurable and one would only need to rewrite Eq. (4.21) in a more convenient form for an application.

Instead, to obtain a measurable angular distribution, we must recast the variables appearing in  $\mathcal{P}(\dots)$  in terms of those defined earlier by Figs. 2 and 3. The final variables are  $\theta_e$ ,  $\phi_e$ ,  $E_1$ ,  $E_2$  and  $\cos\phi$ . We do this in three steps: The first two steps are coordinate rotations in the  $Z^0$  rest frame, and the third step is the necessary summation over  $\pm|\sin\phi|$ .

### D. Completion of the calculation

*Step 1.* We rotate by  $\theta_1$  so that the new  $z$  axis,  $\bar{z}$  is along  $\pi_1^-$ .

This changes the variables *from* the original  $h$  reference system shown in Fig. 16 with  $(x_h, y_h, z_h)$  coordinates *to* the barred reference system of Fig. 17 with  $(\bar{x}, \bar{y}, \bar{z})$  coordinates. Note that  $\bar{z}$  lies in the  $\hat{z}$  direction of Fig. 2.

This means that we specify the initial  $e^-$  beam direction in terms of the final  $\pi_2^-$  direction. So (see fig. 16) we replace  $\Theta_B$ ,  $\Phi_B$  by the polarangle  $\theta_e$  and an associated azimuthal  $\Phi_\pi$  variable. When  $\Phi_\pi = 0$ , the  $e^-$  beam lies in the  $\tau_1^- \pi_1^-$  plane. The formulas for making this change of

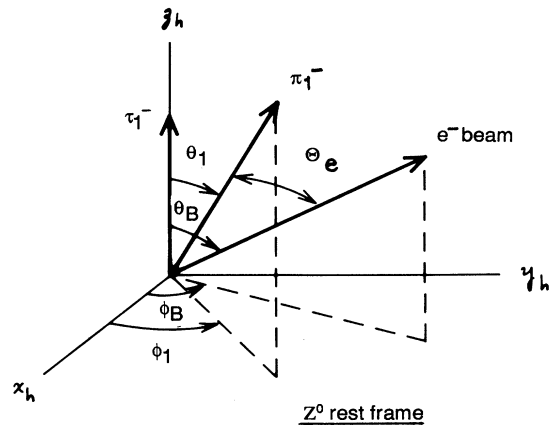


FIG. 16. Angles, needed in the derivation, to describe the  $e^-$  and  $\pi_1^-$  distribution in the  $Z^0$  rest frame, with  $\tau_1^-$  moving in the positive  $z$  direction.

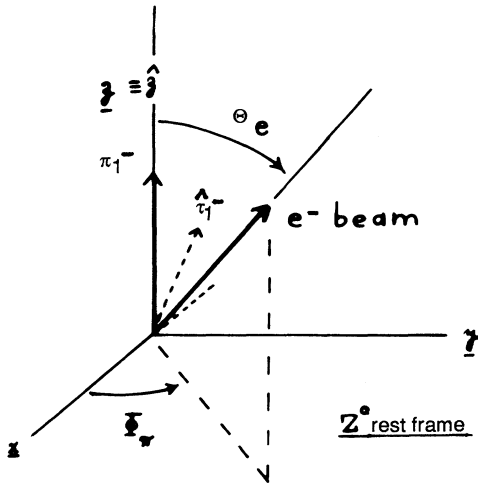


FIG. 17. Barred reference system has  $\pi_1^-$  along the positive  $\bar{z}$  axis with the  $\tau_1^-$  in the negative  $\bar{x}$  half-plane.

variables are

$$\cos\theta_e = \cos\theta_1 \cos\Theta_B + \sin\theta_1 \sin\Theta_B \cos(\Phi_B - \phi_1), \quad (4.23a)$$

$$\begin{aligned} \sin\theta_e \cos\Phi_\pi = & -\sin\theta_1 \cos\Theta_B \\ & + \cos\theta_1 \sin\Theta_B \cos(\Phi_B - \phi_1), \end{aligned} \quad (4.23b)$$

$$\sin\theta_e \sin\Phi_\pi = \sin\Theta_B \sin(\Phi_B - \phi_1). \quad (4.23c)$$

Since this is simply a coordinate rotation,

$$d(\cos\theta_e) d\Phi_\pi = d(\cos\Theta_B) d(\Phi_B - \phi_1). \quad (4.24)$$

So the Jacobian is 1, and  $\cos\theta_e$  and  $\Phi_\pi$  have the usual range for spherical coordinates. Note also that

$$\cos\Theta_B = \cos\theta_1 \cos\theta_e - \sin\theta_1 \sin\theta_e \cos\Phi_\pi. \quad (4.25)$$

The second rotation will make use of the direction of the  $\pi_2^+$  momentum. It was displayed in Fig. 3 in the original  $h$  reference system. See Fig. 18 where the  $\pi_2^+$

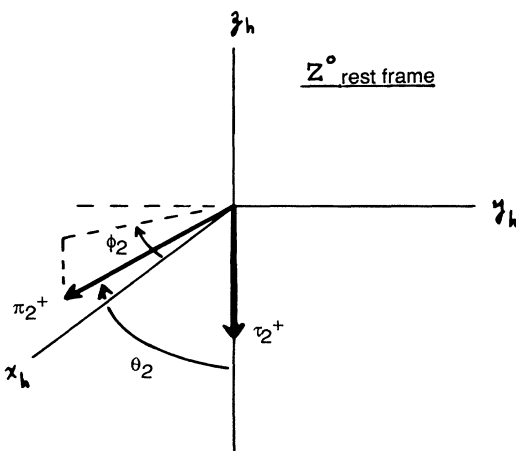


FIG. 18.  $\pi_2^+$  in the original  $h$  reference system.

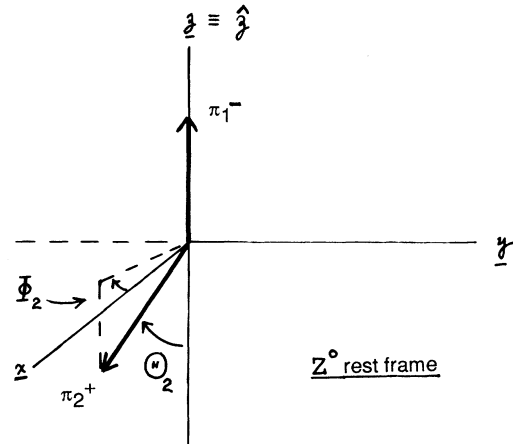


FIG. 19.  $\pi_2^+$  in the barred reference system. The angles  $\Theta_2$  and  $\Phi_2$  are shown. (The  $\cos\Phi_2$  is measurable, but the sign of  $\sin\Phi_2$  is not because of the missing  $v$  and  $\bar{v}$  momenta.)

momentum is shown by itself. By “step 1” we specify the  $\pi_2^+$  in the barred reference system shown in Fig. 19. The  $\pi_2^+$  is at angles  $\Theta_2$  and  $\Phi_2$ . These auxiliary variables are given by

$$\cos\Theta_2 = \cos\theta_1 \cos\theta_2 - \sin\theta_1 \sin\theta_2 \cos\phi, \quad (4.26a)$$

$$\sin\Theta_2 = (1 - \cos^2\Theta_2)^{1/2}, \quad (4.26b)$$

and

$$\sin\Theta_2 \cos\Phi_2 = \sin\theta_1 \cos\theta_1 + \cos\theta_1 \sin\theta_2 \cos\phi, \quad (4.27a)$$

$$\sin\Theta_2 \sin\Phi_2 = \sin\theta_2 \sin\phi. \quad (4.27b)$$

Note from Eq. (4.27b) that the sign ambiguity in  $\sin\phi$  induces a corresponding sign ambiguity in  $\sin\Phi_2$ .

These auxiliary variables  $\cos\Phi_2$  and  $\sin\Phi_2$  will appear in the various BRSC functions later on in this paper in order to shorten those expressions.

Step 2: We rotate by  $-\Phi_2$  about  $\bar{z}=\hat{z}$  so that  $\pi_2^+$  is in the positive  $\hat{x}$  plane.

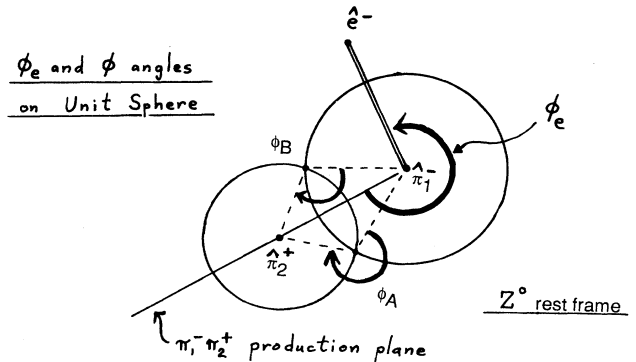


FIG. 20. Summary illustration on the unit sphere showing the azimuthal angles  $\phi_e$  and  $\phi$ , as well as the polar angle  $\theta_e$ . Note that  $\cos\phi = \cos\phi_A = \cos\phi_B$ . See Fig. 13 and its caption for how the radii of the two circles can be obtained.

This changes the variables from the barred reference system of Fig. 17 to the desired  $\pi_1^-$  reference system of Fig. 2 with  $(\hat{x}, \hat{y}, \hat{z})$  coordinates. By this rotation,

$$\phi_e = \Phi_\pi + \Phi_2 \quad (4.28)$$

The Jacobian is 1, and  $\phi_e$  has the full  $2\pi$  range,  $-\pi \leq \phi_e \leq \pi$ .

In Fig. 20 the important angles  $\phi_e$  and  $\phi$  are shown, along with  $\theta_e$  on the unit sphere.

*Step 3:* The sum over  $\pm|\sin\phi|$  is performed.

This summation discards those terms linear in  $\sin\phi$  or in  $\sin\Phi_2$ .

### E. Result

The result then is the full beam-referenced spin-correlation function

$$I(\theta_e, \phi_e, E_1, E_2, \phi) = \sum_r \mathcal{P}_r \mathcal{A}_r(E_1, E_2), \quad (4.29)$$

where  $r=0, 1, \kappa, \kappa'$ . The  $Z^0$  decay analyzer coefficients are

$$\begin{aligned} \mathcal{A}_0 &= (1-\delta)(1 + \cos\theta_1^\tau \cos\theta_2^\tau) + \alpha(\cos\theta_1^\tau + \cos\theta_2^\tau), \\ \mathcal{A}_1 &= (1-\delta)(\cos\theta_1^\tau + \cos\theta_2^\tau) + \alpha(1 + \cos\theta_1^\tau \cos\theta_2^\tau), \\ \mathcal{A}_\kappa &= -\kappa \sin\theta_1^\tau \sin\theta_2^\tau, \\ \mathcal{A}_{\kappa'} &= -\kappa' \sin\theta_1^\tau \sin\theta_2^\tau, \end{aligned} \quad (4.30)$$

where the  $Z^0$  decay intensity parameters  $(\delta, \alpha, \kappa, \kappa')$  have been defined in Sec. II. The  $Z^0$  production coefficients are

$$\begin{aligned} \mathcal{P}_0 &= 2 + 2 \cos^2\theta_1 \cos^2\theta_e + \sin^2\theta_1 \sin^2\theta_e - 2 \cos\phi_e \sin 2\theta_e \sin\theta_1 \cos\theta_1 \cos\Phi_2 + \cos 2\phi_e \sin^2\theta_e \sin^2\theta_1 \cos 2\Phi_2, \\ \mathcal{P}_1 &= 4 \frac{T_e}{S_e} (\cos\theta_1 \cos\theta_e - \cos\phi_e \sin\theta_1 \sin\theta_e \cos\Phi_2), \\ \mathcal{P}_\kappa &= \sin^2\theta_1 \cos\phi (3 \cos^2\theta_e - 1) + 2 \cos\phi_e \sin 2\theta_e \sin\theta_1 (\sin\Phi_2 \sin\phi + \cos\theta_1 \cos\Phi_2 \cos\phi) \\ &\quad + \cos 2\phi_e \sin^2\theta_e [2 \cos\theta_1 \sin 2\Phi_2 \sin\phi + (1 + \cos^2\theta_1) \cos 2\Phi_2 \cos\phi], \\ \mathcal{P}_{\kappa'} &= 2 \sin\phi_e \sin 2\theta_e \sin\theta_1 (\cos\Phi_2 \cos\phi + \cos\theta_1 \sin\Phi_2 \sin\phi) + \sin 2\phi_e \sin^2\theta_e [2 \cos\theta_1 \cos 2\Phi_2 \cos\phi + (1 + \cos^2\theta_1) \sin 2\Phi_2 \sin\phi]. \end{aligned} \quad (4.31)$$

The total number of events is then

$$(\text{No. of events}) = \text{const} \times \int_0^\pi d\phi \int_{-\pi}^\pi d\phi_e \int_{-1}^1 d(\cos\theta_e) \int_{-1}^1 d(\cos\theta_1^\tau) \int_{-1}^1 d(\cos\theta_2^\tau) I(\theta_e, \phi_e, E_1, E_2, \phi). \quad (4.32)$$

The result is quadratic in the  $e^-e^+ \rightarrow Z^0$  formation amplitudes  $\tilde{T}(s_1 s_2)$ , since the parameters  $S_e$  and  $T_e$  are

$$\begin{aligned} S_e &\equiv |\tilde{T}(-+)|^2 + |\tilde{T}(+-)|^2 \rightarrow (1 + |r_e|^2) M^2, \\ T_e &\equiv |\tilde{T}(+-)|^2 - |\tilde{T}(-+)|^2 \rightarrow -(r_e + r_e^*) M^2. \end{aligned} \quad (4.33)$$

These  $S_e$  and  $T_e$  are simply  $e^-e^+ \rightarrow Z^0$  formation intensity parameters. Since there is a spin-correlation effect in the final state, Eq. (4.29) does not factor into a production times a decay part. Instead,  $I(\dots)$  consists of the sum of factoring terms.

### F. $I(\theta_e, E_1, E_2, \phi)$ beam-referenced spin-correlation function

If the azimuthal angle of the  $e^-$  beam, the angle  $\phi_e$ , is integrated over, from Eq. (4.29), we obtain

$$\begin{aligned} I(\theta_e, E_1, E_2, \phi) &= (2 + 2 \cos^2\theta_1 \cos^2\theta_e + \sin^2\theta_1 \sin^2\theta_e) [(1-\delta)(1 + \cos\theta_1^\tau \cos\theta_2^\tau) + \alpha(\cos\theta_1^\tau + \cos\theta_2^\tau)] \\ &\quad + 4 \frac{T_e}{S_e} \cos\theta_1 \cos\theta_e [(1-\delta)(\cos\theta_1^\tau + \cos\theta_2^\tau) + \alpha(1 + \cos\theta_1^\tau \cos\theta_2^\tau)] - \kappa \sin^2\theta_1 (3 \cos^2\theta_e - 1) \sin\theta_1^\tau \sin\theta_2^\tau \cos\phi. \end{aligned} \quad (4.34)$$

However, there is a more direct route to obtain Eq. (4.34). After step 1, we simply integrate Eq. (4.20) over the azimuthal angle  $\Phi_\pi$  and sum over  $\pm|\sin\phi|$ .

In Appendix B we discuss how from Eq. (4.34) one can obtain other asymmetry functions and correlation functions for  $e^-e^+$  collisions producing  $\tau^-\tau^+$  at the  $Z^0$  or at a more massive  $Z'$ .

### V. AZIMUTHAL CORRELATION FUNCTION $I(\phi_e, \phi)$

In this section, from Eq. (4.29), we obtain the azimuthal correlation function  $I(\phi_e, \phi)$ . The  $\theta_e$  variable is easily integrated out to give

$$I(\phi_e, \phi) = L(\phi_e, \phi) + \kappa' K'(\phi_e, \phi), \quad (5.1)$$

where

$$\begin{aligned} L(\phi_e, \phi) = & \frac{16}{3} \int_{-1}^1 d(\cos\theta_1^\tau) \int_{-1}^1 d(\cos\theta_2^\tau) \mathcal{A}_0 + \frac{4}{3} \cos 2\phi_e \int_{-1}^1 d(\cos\theta_1^\tau) \int_{-1}^1 d(\cos\theta_2^\tau) \sin^2\theta_1 \cos 2\Phi_2 \mathcal{A}_0 \\ & - \left[ \frac{2\pi T_e}{S_e} \right] \cos\phi_e \int_{-1}^1 d(\cos\theta_1^\tau) \int_{-1}^1 d(\cos\theta_2^\tau) \sin\theta_1 \cos\Phi_2 \mathcal{A}_1 \\ & + \frac{4}{3} \kappa \cos 2\phi_e \int_{-1}^1 d(\cos\theta_1^\tau) \int_{-1}^1 d(\cos\theta_2^\tau) [2 \cos\theta_1 \sin 2\Phi_2 \sin\phi + (1 + \cos^2\theta_1) \cos 2\Phi_2 \cos\phi] \overline{\mathcal{A}}_\kappa, \end{aligned} \quad (5.2a)$$

and

$$K'(\phi_e, \phi) = \frac{4}{3} \sin 2\phi_e \int_{-1}^1 d(\cos\theta_1^\tau) \int_{-1}^1 d(\cos\theta_2^\tau) [2 \cos\theta_1 \cos 2\Phi_2 \cos\phi + (1 + \cos^2\theta_1) \sin 2\Phi_2 \sin\phi] \overline{\mathcal{A}}_{\kappa'}. \quad (5.2b)$$

The associated  $\kappa'$  analyzing-power function is

$$R(\phi_e, \phi) \equiv \frac{K'(\phi_e, \phi)}{L(\phi_e, \phi)}. \quad (5.3)$$

The decay analyzer coefficients were listed before in Eq. (4.30) except that now the barred ones have their intensity parameters removed: i.e.,

$$\overline{\mathcal{A}}_\kappa = \overline{\mathcal{A}}_{\kappa'} = -\sin\theta_1^\tau \sin\theta_2^\tau. \quad (5.4)$$

Similarly, the  $(1-\delta)$  and  $\alpha$  intensity parameters can be easily isolated in Eq. (5.2a), and also in Eq. (4.29), by rearranging the  $\mathcal{A}_0$  and  $\mathcal{A}_1$  terms.

The folded one-variable distributions  $I_{\lessgtr}(\phi)$  are obtained by integrating Eq. (5.1) over the  $\phi_e$  variable:

$$I_{>}(\phi) = L(\phi) + \kappa' K'(\phi) = \int_0^{\pi/2} d\phi_e I(\phi_e, \phi), \quad (5.5)$$

and

$$I_{<}(\phi) = L(\phi) - \kappa' K'(\phi) = \int_{-\pi/2}^0 d\phi_e I(\phi_e, \phi), \quad (5.6)$$

where

$$\begin{aligned} L(\phi) = & 1 - \delta - \frac{3}{16} \frac{T_e}{S_e} \int_{-1}^1 d(\cos\theta_1^\tau) \int_{-1}^1 d(\cos\theta_2^\tau) \mathcal{A}_1 \sin\theta_1 \cos\Phi_2, \\ \mathcal{A}_1 = & (1 - \delta)(\cos\theta_1^\tau + \cos\theta_2^\tau) + \alpha(1 + \cos\theta_1^\tau \cos\theta_2^\tau), \end{aligned} \quad (5.7)$$

with

$$K'(\phi) = \frac{1}{8\pi} \int_{-1}^1 d(\cos\theta_1^\tau) \int_{-1}^1 d(\cos\theta_2^\tau) [2 \cos\theta_1 \cos 2\Phi_2 \cos\phi + (1 + \cos^2\theta_1) \sin 2\Phi_2 \sin\phi] \overline{\mathcal{A}}_{\kappa'}, \quad (5.8)$$

with  $\overline{\mathcal{A}}_{\kappa'}$  given in Eq. (5.4). With  $I(\phi)$  the associated  $\kappa'$  analyzing-power function is

$$R(\phi) \equiv \frac{K'(\phi)}{L(\phi)}. \quad (5.9)$$

The auxiliary variable  $\Phi_2$  which appears in these equations for  $I(\phi_e, \phi)$  and for  $I(\phi)$  is defined by Eqs. (4.26) and (4.27).

### VI. GENERALIZATION TO INCLUDE THE $\tau$ DECAY CHIRALITY PARAMETER $\xi$ AND TO OTHER $\tau$ DECAY MODES

By a simple  $\xi\mathcal{S}$ -substitution rule, one can easily generalize any of the above  $I(\dots)$  functions to those for the production-decay sequence

$$e^- e^+ \rightarrow Z^0 \rightarrow \tau_1^- \tau_2^+ \rightarrow (h_1^- \nu)(h_2^+ \bar{\nu}).$$



For  $\tau \rightarrow h\nu$  the hadrons considered are  $h = \pi, K, \rho, K^*$ , and  $a_1^{\text{ch}}$ . The notation  $a_1^{\text{ch}}$  denotes the decay  $\tau^- \rightarrow \pi^- \pi^+ \pi^- \nu$  assuming that it is dominated by the spin-1  $a_1$  resonance, as expected. See the ARGUS Collaboration result of Ref. 12.

There are two parameters to be inserted in the equations for  $I(\dots)$ . The chirality parameter  $\xi$  was explained in Eq. (1.2) in the Introduction.

The other additional parameter  $\mathcal{S}_h$  has the following values when  $\tau^- \rightarrow h^- \nu$ :

$$\mathcal{S}_h = \begin{cases} 1 & \text{for } h = \pi, K, \\ \frac{m_\tau^2 - 2m_h^2}{m_\tau^2 + 2m_h^2} & \text{for } h = \rho, K^*, a_1. \end{cases} \quad (6.1)$$

This  $\mathcal{S}_h$  parameter we call the ‘‘hadron helicity parameter’’ since it characterizes the effective hadron helicity of the  $\tau^- \rightarrow h^- \nu$  coupling in the pure  $V - A$  limit. That is, for  $\xi_h = 1$ , when  $\mathcal{S}_h = 1$ , only helicity 0 hadrons couple in  $\tau^- \rightarrow h^- \nu$ , and if (unphysically)  $\mathcal{S}_h = -1$ , only helicity  $-1$  hadrons would be coupled. When  $\mathcal{S}_h = 0$ , which is almost true for the  $a_1$ , there is an equal probability that a helicity 0 and  $-1$  hadron is coupled. Numerically,

$$\begin{aligned} \mathcal{S}_\rho &= 0.457, \\ \mathcal{S}_{K^*} &= 0.333, \\ \mathcal{S}_{a_1} &= -0.011. \end{aligned}$$

When respect to using spin-correlation effects via a BRSC function in the analysis of event distributions, it is the unequal average amounts of helicity 0 and  $-1$  hadrons in  $\tau^- \rightarrow h\nu$  which are responsible for the spin-correlation effect when the coupling is  $V - A$ . Therefore,  $\mathcal{S}_h$  actually acts as a suppression factor.

#### A. $\xi\mathcal{S}$ -substitution rule

The BRSC function derived in Sec. IV for the spectrum  $\{\pi_1^- \pi_2^+\}$  can be very simply generalized to the spectrum  $\{h_1^- h_2^+\}$ , where each  $\tau$  decays in a two-body mode and  $h_{12}^{\pm} = \pi, K, \rho, K^*, a_1$  by using a  $\xi\mathcal{S}$  substitution rule: Replace

$$\begin{aligned} \cos\theta_1^\tau &\rightarrow \xi_1 \mathcal{S}_1 \cos\theta_1^\tau, \\ \sin\theta_1^\tau &\rightarrow \xi_1 \mathcal{S}_1 \sin\theta_1^\tau, \end{aligned} \quad (6.2)$$

and likewise for  $\cos\theta_2^\tau$  and  $\sin\theta_2^\tau$ .

It is to be understood that the angle variables without  $\tau$  superscripts are *not* to be replaced. So this only affects the  $\mathcal{A}$  coefficients and not the  $\mathcal{P}$  coefficients.

The origin of this useful rule is the form of the two-body  $\tau$  decay density matrices, plus the structure of the derivation of these various spin-correlation functions:

For  $h$  with spin 0, e.g.,  $\tau_1^- \rightarrow \pi_1^- \nu$ , when we allow for a neutrino with helicity  $\mu_2$ , the helicity amplitude  $C(0, \mu_2)$  is defined by

$$\langle \theta_1^\tau, \phi_1, 0, \mu_2 | \frac{1}{2}, \lambda_1 \rangle = D_{\lambda_1, -\mu_2}^{1/2*}(\phi_1, \theta_1^\tau - \phi_1) C(0, \mu_2). \quad (6.3)$$

The associated density matrix then is

$$\rho_{\lambda_1 \lambda_1'}(\tau_1^- \rightarrow \pi_1^- \nu) = \sum_{\mu_2 = \mp 1/2} D_{\lambda_1, -\mu_2}^{1/2*} D_{\lambda_1', -\mu_2}^{1/2} |C(0, \mu_2)|^2 \quad (6.4a)$$

$$= \frac{1}{2} (|g_L|^2 + |g_R|^2) e^{i(\lambda_1 - \lambda_1')\phi_1} \begin{bmatrix} 1 + \xi_\pi \cos\theta_1^\tau & \xi_\pi \sin\theta_1^\tau \\ \xi_\pi \sin\theta_1^\tau & 1 - \xi_\pi \cos\theta_1^\tau \end{bmatrix}, \quad (6.4b)$$

where

$$\xi_\pi = \frac{|C(0, -\frac{1}{2})|^2 - |C(0, \frac{1}{2})|^2}{|C(0, -\frac{1}{2})|^2 + |C(0, \frac{1}{2})|^2} \quad (6.5a)$$

$$= \frac{|g_L|^2 - |g_R|^2}{|g_L|^2 + |g_R|^2}. \quad (6.5b)$$

For  $\tau_2^+ \rightarrow \pi_2^+ \bar{\nu}$ , in Eq. (6.4b) simply replace  $\lambda_1 \rightarrow \lambda_2$ ,  $\lambda_1' \rightarrow \lambda_2'$ , and change  $\xi_\pi \rightarrow -\xi_\pi$ .

For spin 1, e.g.,  $\tau^- \rightarrow \rho^- \nu$ , instead,

$$\langle \theta_1^\tau, \phi_1, \mu_1, \mu_2 | \frac{1}{2}, \lambda_1 \rangle = D_{\lambda_1, \mu}^{1/2*}(\phi_1, \theta_1^\tau, -\phi_1) T(\mu_1, \mu_2), \quad (6.6)$$

where  $\mu = \mu_1 - \mu_2$ , and so

$$\rho_{\lambda_1 \lambda_1'}(\tau_1^- \rightarrow \rho_1^- \nu) = \frac{1}{2} \left[ \sum_{\mu_1 \mu_2} |T(\mu_1, \mu_2)|^2 \right] e^{i(\lambda_1 - \lambda_1')\phi_1} \begin{bmatrix} 1 + \xi_\rho \mathcal{S}_\rho \cos\theta_1^\tau & \xi_\rho \mathcal{S}_\rho \sin\theta_1^\tau \\ \xi_\rho \mathcal{S}_\rho \sin\theta_1^\tau & 1 - \xi_\rho \mathcal{S}_\rho \cos\theta_1^\tau \end{bmatrix}, \quad (6.7)$$

where

$$\xi_\rho \mathcal{S}_\rho \equiv \frac{|T(0, -\frac{1}{2})|^2 - |T(-1, -\frac{1}{2})|^2 + |T(1, \frac{1}{2})|^2 - |T(0, \frac{1}{2})|^2}{|T(0, -\frac{1}{2})|^2 + |T(-1, -\frac{1}{2})|^2 + |T(1, \frac{1}{2})|^2 + |T(0, \frac{1}{2})|^2}. \quad (6.8)$$

TABLE V. Comparison of ideal statistical errors for  $\sin^2\theta_W$  from measurements by the full beam-referenced  $\tau$  spin-correlation function  $I(\theta_e, \phi_e, E_1, E_2, \phi)$  with measurements by the energy-correlation function  $I(E_1, E_2)$  for the production-decay sequence  $e^-e^+ \rightarrow Z^0 \rightarrow \tau_1^- \tau_2^+ \rightarrow (h_1^- \nu)(h_2^+ \bar{\nu})$ . Superscripts denote the smallest ideal statistical errors which can be obtained from a single decay mode.  $10^7 Z^0$  events have been assumed. For the reader's convenience, the equivalent error to  $\sigma(\sin^2\theta_W)$  is listed for  $A_{LR} \simeq -\alpha_H \simeq 2av/(a^2+v^2)$ , where  $a, v$  describe  $Z^0 \rightarrow \tau^- \tau^+$  at the tree level.  $A_{LR}$  is the initial-state longitudinal-polarization asymmetry in muon-pair production by a longitudinally polarized  $e^-$  beam in  $e^-e^+$  annihilation.

Sequential decay mode	Number of events	Comparison of ideal statistical errors			
		$\sigma(\sin^2\theta_W)$ $I(\theta_e, \phi_e, E_1, E_2, \phi)$	$I(E_1, E_2)$	$\sigma(\alpha_H \simeq -A_{LR})$ $I(\theta_e, \phi_e, E_1, E_2, \phi)$	$I(E_1, E_2)$
$(\pi, K)^-(\pi, K)^+$	4377	$0.199 \times 10^{-2}$	$0.261 \times 10^{-2}$	0.0156	0.0205
$(\pi, K)^-\rho^+$	17129	$0.121 \times 10^{-2a}$	$0.159 \times 10^{-2a}$	0.00948 <sup>a</sup>	0.0124 <sup>a</sup>
$(\pi, K)^-K^{*+}$	1066	$0.495 \times 10^{-2}$	$0.652 \times 10^{-2}$	0.0389	0.0511
$(\pi, K)^-a_1^{\text{ch}+}$	5101	$0.233 \times 10^{-2}$	$0.307 \times 10^{-2}$	0.0183	0.0241
$\rho^-\rho^+$	16757	$0.192 \times 10^{-2}$	$0.271 \times 10^{-2}$	0.0150	0.0213
$\rho^-K^{*+}$	2085	$0.595 \times 10^{-2}$	$0.871 \times 10^{-2}$	0.0467	0.0684
$\rho^-a_1^{\text{ch}+}$	9980	$0.310 \times 10^{-2}$	$0.482 \times 10^{-2}$	0.0243	0.0379
$K^{*-}K^{*+}$	65	$3.805 \times 10^{-2}$	$5.905 \times 10^{-2}$	0.2986	0.4634
$K^{*-}a_1^{\text{ch}+}$	621	$1.473 \times 10^{-2}$	$2.654 \times 10^{-2}$	0.1156	0.2083
Sum of above modes	57181	$0.0798 \times 10^{-2}$ factor worse = 1.34	$0.107 \times 10^{-2}$	0.00626	0.00841 factor worse = 1.34

<sup>a</sup>Smallest.

For  $\tau_2^+ \rightarrow \rho^+ \bar{\nu}$  the analog to Eq. (6.7) has  $\lambda_1 \rightarrow \lambda_2$ ,  $\lambda'_1 \rightarrow \lambda'_2$ , and  $\xi_\rho \rightarrow -\xi_\rho$ .

From Eqs. (6.4) and (6.7), plus the structure of the derivation in Sec. IX, the  $\xi\mathcal{S}$ -substitution rule follows.

### VII. IDEAL STATISTICAL ERRORS FOR A $10^7 Z^0$ EVENT SAMPLE

We consider a  $10^7 Z^0$  event sample and assume a  $Z^0 \rightarrow \tau^- \tau^+$  branching ratio of 3.31%. For other choices any of the ideal statistical errors listed here can be rescaled. We take all  $\tau$  into one-charged-particle branching ratios from the tabulation of Hayes and Perl<sup>25</sup> except that for  $\tau^- \rightarrow a_1^{\text{ch}-} \nu$  with  $a_1^{\text{ch}-} \rightarrow \pi^- \pi^+ \pi^-$  we use the ‘‘formal average’’ listed by Gan and Perl in Ref. 26.

Using the full BRSC function of Eq. (4.29) for the production-decay sequence

$$e^-e^+ \rightarrow Z^0 \rightarrow \tau_1^- \tau_2^+ \rightarrow (h_1^- \nu)(h_2^+ \bar{\nu}), \quad (7.1)$$

we have calculated the associated ‘‘ideal statistical errors’’ for a least-squares measurement of the three parameters  $\sin^2\theta_W$ , the chirality parameter  $\xi_1$  for  $\tau_1^- \rightarrow h_1^- \nu$ , and the chirality parameter  $\xi_2$  for  $\tau_2^+ \rightarrow h_2^+ \bar{\nu}$ . In calculating the errors for  $\sin^2\theta_W$ , we assume lepton universality with  $S_e$  and  $T_e$ , and the  $Z$  decay intensity parameters

all depending on  $\sin^2\theta_W$ . Our procedure is ‘‘ideal’’ in that we do not, unlike in a Monte Carlo simulation, include the statistical error from a presumably Poisson distribution of data in each bin instead of the ‘‘theorist’s ideal distribution’’ according to Eq. (4.29). It is also ideal in that we sum over modes to compute a formal average, whereas the Particle Data Group’s method is to first combine the systematic and statistical errors in quadrature.

The BRSC function of Eq. (4.29) is asymmetric in appearance with respect to the treatment of the final particles  $h_1^-$  and  $h_2^+$ . This arises because  $\theta_1$ , and not  $\theta_2$ , appears on the right-hand side of Eq. (4.29). However, we find the same numerical  $\sigma(\xi_{h_1})$  errors for  $\{h_1^- h_2^+\}$  and for  $\{h_2^+ h_1^-\}$ , and so we have combined the errors in quadrature to obtain  $\sigma(\xi_{h_1})$  in the tabulation in the tables. The same is true for  $\sigma(\sin^2\theta_W)$ .

The results for  $\sin^2\theta_W$  are listed<sup>27</sup> in Table V. For comparison purposes we have also tabulated the corresponding ideal statistical error for measurement using the simpler energy-correlation function  $I(E_1, E_2)$ , which is discussed in Ref. 10. Also, for comparison and as a check, for three of the modes we list in Table VI the results for  $I(\theta_e, E_1, E_2, \phi)$  versus the full BRSC function  $I(\theta_e, \phi_e, E_1, E_2, \phi)$ .

TABLE VI. Comparison of ideal statistical errors  $\sigma(\sin^2\theta_W)$  as obtained from the full BRSC function,  $I(\theta_e, \phi_e, E_1, E_2, \phi)$  with those from  $I(\theta_e, E_1, E_2, \phi)$ .

Sequential decay mode	Number of events	Comparison of ideal statistical errors	
		$\sigma(\sin^2\theta_W)$ $I(\theta_e, \phi_e, E_1, E_2, \phi)$	$I(\theta_e, E_1, E_2, \phi)$
$(\pi^- K)^-(\pi, K)^+$	4377	$0.199 \times 10^{-2}$	$0.202 \times 10^{-2}$
$(\pi^- K)^-\rho^+$	17129	$0.121 \times 10^{-2}$	$0.121 \times 10^{-2}$
$\rho^-\rho^+$	16757	$0.192 \times 10^{-2}$	$0.192 \times 10^{-2}$

TABLE VII. Comparison of ideal statistical errors for the chirality parameter  $\xi_\pi$  from measurements by the full BRSC function with those from measurements by  $I(E_\pi, E_B)$ . For the standard  $V-A$  coupling in  $\tau^- \rightarrow \pi^- \nu$  decay,  $\xi_\pi = 1$ .

Sequential ( $\pi, K$ ) $^- B^+$ mode	$I(\theta_e, \phi_e, E_\pi, E_B, \phi)$ $\sigma(\xi_\pi)$	$I(E_\pi, E_B)$ $\sigma(\xi_\pi)$
$B$ particle		
( $\pi, K$ ) $^+$	0.0122	0.0157
$\rho^+$	0.0328	0.0410
$K^{*+}$	0.1650	0.2086
$a_1^{\text{ch}+}$	0.1173	0.1512
Sum of above modes	0.0114	0.0146
		factor worse=1.28

Tables VII–IX, respectively, continue the comparison between the full BRSC function and the energy-correlation function, but in terms of the determination of the hadronic  $\tau$  decay chirality parameters  $\xi_\pi$ ,  $\xi_\rho$ , and  $\xi_{K^*}$ . Before,<sup>10</sup> from  $I(E_1, E_2)$ , we found that by a one-parameter fit the ideal statistical percentage error in the determination of the Michel parameter  $\xi$  is 2.9%; and of the chirality parameters is for  $\xi_\pi$ , 1.3% (here the  $\pi$  and  $K$  modes have been combined); for  $\xi_\rho$ , 3.08%; and for  $\xi_{K^*}$ , 18%. (For  $a_1^{\text{ch}}$ , since  $\mathcal{S}_{a_1} \sim 0.0$ , the associated  $\xi_{a_1}$  chirality parameter cannot be accurately determined by this technique.) These  $\sigma$ 's involved a sum over modes.

### VIII. CONCLUSIONS

(1) The beam-referenced spin-correlation functions for production-decay sequence

$$e^-e^+ \rightarrow Z^0 \rightarrow \tau^- \tau^+ \rightarrow (h_1^- \nu)(h_2^+ \bar{\nu}), \quad (8.1)$$

at the  $Z^0$  resonance, are easily derived using the helicity formalism. For  $\tau_1^- \rightarrow \pi_1^- \nu$ , for example, this reaction is

TABLE VIII. Comparison of ideal statistical errors for the chirality parameter  $\xi_\rho$  from measurements by the full BRSC function with those from measurements by  $I(E_\rho, E_B)$ . For the standard  $V-A$  coupling in  $\tau^- \rightarrow \rho^- \nu$  decay,  $\xi_\rho = 1$ .

Sequential $\rho^- B^+$ mode	$I(\theta_e, \phi_e, E_\rho, E_B, \phi)$ $\sigma(\xi_\rho)$	$I(E_\rho, E_B)$ $\sigma(\xi_\rho)$
$B$ particle		
( $\pi, K$ ) $^+$	0.0385	0.0472
$\rho^+$	0.0416	0.0517
$K^{*+}$	0.2672	0.3344
$a_1^{\text{ch}+}$	0.1870	0.2378
Sum of above modes	0.0278	0.0343
		factor worse=1.23

TABLE IX. Comparison of ideal statistical errors for the chirality parameter  $\xi_{K^*}$  from measurements by the full BRSC function with those from measurements by  $I(E_{K^*}, E_B)$ . For the standard  $V-A$  coupling in  $\tau^- \rightarrow K^{*-} \nu$  decay,  $\xi_{K^*} = 1$ .

Sequential $K^{*-} B^+$ mode	$I(\theta_e, \phi_e, E_{K^*}, E_B, \phi)$ $\sigma(\xi_{K^*})$	$I(E_{K^*}, E_B)$ $\sigma(\xi_{K^*})$
$B$ particle		
( $\pi, K$ ) $^+$	0.217	0.2646
$\rho^+$	0.300	0.3734
$K^{*+}$	1.179	1.474
$a_1^{\text{ch}+}$	1.031	1.309
Sum of above modes	0.171	0.2108
		factor worse=1.23

analyzed relative to the final  $\pi^-$  momentum vector as shown in Fig. 2.

(2) In spite of the missing  $\nu$  and  $\bar{\nu}$  momenta, events for production-decay sequences can be easily recorded in terms of the  $\theta_e$  and  $\phi_e$  angles, the  $h_1^-$  energy  $E_1$ , the  $h_2^+$  energy  $E_2$ , and the cosine of the angle  $\phi$  between the  $\tau_1^- \rightarrow h_1^- \nu$  and  $\tau_2^+ \rightarrow h_2^+ \bar{\nu}$  decay planes. These are all measurable quantities in the  $Z^0$  rest frame. Since the  $h_1^-$  energy  $E_1$  is equivalent to the  $\theta_1^\tau$  angle of the  $h_1$  in the  $\tau_1^-$  rest frame, and analogously  $E_2$  is equivalent to the  $\theta_2^\tau$  angle in the  $\tau_2^+$  rest frame, the power of the helicity approach can be easily exploited for simple spin-correlation analyses of such production-decay sequences. For the reaction in Eq. (8.1) and, more generally, for  $e^-e^+ \rightarrow \tau^- \tau^+$ , the directions for the missing  $\nu_\tau$  and  $\bar{\nu}_\tau$  are known up to a twofold kinematic ambiguity.

(3) Using the full BRSC function for  $10^7 Z^0$  events, the ideal statistical error in the determination of  $\sin^2 \theta_W$  is  $0.8 \times 10^{-3}$  when the  $\{h_1^-, h_2^+\}$  channels are summed over where  $h = \pi, \kappa, \rho, K^*, a_1^{\text{ch}}$ . The best individual mode is  $\{(\pi, K)^- \rho^+\}$ , for which  $\sigma(\sin^2 \theta_W) = 1.2 \times 10^{-3}$ . This is only a 25% reduction in the ideal statistical errors, which were obtained in Ref. 3 from the simpler energy-correlation function for hadronic  $\tau$  decays. However, usage of the azimuthal correlations in, for instance,  $I(\phi_e, \phi)$  may help in controlling systematic errors. There is a similar, but smaller, reduction in the ideal statistical errors for the chirality parameters  $\xi_\pi$ ,  $\xi_\rho$ , and  $\xi_{K^*}$  when the full BRSC function is used instead of  $I(E_1, E_2)$ .

(4) Measurement of the  $Z^0 \rightarrow \tau^- \tau^+$  decay intensity parameters  $(\delta, \alpha, \kappa, \kappa')$  will completely determine the fundamental helicity amplitudes  $T(-+)$  and  $T(+)$ .

(5) The most interesting result is that an azimuthal correlation function  $I(\phi_e, \phi)$  can be simply used to test for maximal  $P$ , maximal  $C$  violation in the  $Z^0 \rightarrow \tau^- \tau^+$  coupling. The explicit  $\phi_e$  and  $\phi$  distribution of  $I(\phi_e, \phi)$  and of the associated  $\kappa'$  analyzing power  $R(\phi_e, \phi)$  is given in Figs. 4 and 8 and, analytically, in Eqs. (5.1)–(5.9).

This observable  $I(\phi_e, \phi)$ , can also be used for leptonic  $\tau$  decay modes. For the  $\{l_1^- h_2^+\}$  and  $\{l_1^- l_2^+\}$  sequential

decay channels, an odd  $\phi_e$  component in  $I(\phi_e, \phi)$  would indicate a violation of time-reversal invariance if a first-order Hermitian Hamiltonian is assumed.

(6) For  $e^-e^+$  collisions in the  $\Upsilon$  or  $J/\psi$  regions, the  $\phi_e$  behavior of  $I(\phi_e, \phi)$  can be used to test for a complex phase in the  $\gamma^* \rightarrow \tau^- \tau^+$  coupling. Assuming a first-order Hermitian effective Hamiltonian,  $I(\phi_e, \phi)$  tests for a violation of time-reversal invariance.

We hope that the material in this paper will help in the evaluation of when to include, and when not to include, the  $\theta_e$  and  $\phi_e$ , and  $\phi$  dependence in spin-correlation analyses for production-decay sequences in unpolarized  $e^-e^+$  collisions.

#### ACKNOWLEDGMENTS

For informative and helpful discussions on  $\tau$  physics and on  $\tau$ -pair Monte Carlo studies, the author thanks S. Jadach and Z. Was, and he thanks Stephen Goozov for help with the computer analysis and for checking some of the material. He thanks LEP experimentalists for helpful discussions, and thanks the theory groups at CERN and Cornell for their hospitality and intellectual stimulation. This work was completed at CERN and was partially supported by the U.S. Department of Energy, Contract No. DE-FG02-86ER40291.

#### APPENDIX A: CALCULATION OF STANDARD-MODEL $Z^0 \rightarrow \tau^- \tau^+$ HELICITY AMPLITUDES WITH JACOB-WICK PHASE CONVENTION

Central to any spin-correlation effect, such as that of a BRSC function, is a careful and systematic treatment of the quantum-mechanical phases of the basic amplitudes. In part because of its convenience and great versatility, we have assumed the Jacob-Wick phase convention<sup>16</sup> in our derivations. In this appendix we explain how we calculate the  $Z^0 \rightarrow \tau^- \tau^+$  helicity amplitudes in the standard model with this phase convention.

As before in Eq. (4.2), *except that in this appendix we will use lower-case Greek letters without subscripts for the  $\tau_1^-$  angles, the matrix element describing  $Z^0 \rightarrow \tau_1^- \tau_2^+$  is*

$$\langle \theta, \phi, \lambda_1, \lambda_2 | 1 M \rangle = D_{M\lambda}^{1*}(\phi, \theta, -\phi) T(\lambda_1, \lambda_2), \quad (\text{A1})$$

where  $\lambda_1$  denotes the helicity of the  $\tau_1^-$ , and  $\lambda_2$  that of the  $\tau_2^+$ ,  $\lambda = \lambda_1 - \lambda_2$ . The angles  $\theta$  and  $\phi$  are, respectively, the usual polar and azimuthal angles of the  $\tau_1^-$  momentum (see Fig. 14). The  $z$  axis is the  $Z^0$  polarization axis for the eigenstates  $|1 M\rangle$  of Eq. (A1).

We do not calculate Eq. (A1) directly in the standard model, but instead we calculate the corresponding density matrix for the  $Z^0$  eigenstate with  $M=0$ , i.e.,  $|J=1, M=0\rangle$ . From Eq. (A1) these density matrix elements are

$$\begin{aligned} \rho_{\lambda_1 \lambda_2; \lambda'_1 \lambda'_2} &= T(\lambda_1, \lambda_2) T^*(\lambda'_1, \lambda'_2) D_{0\lambda}^{1*}(\phi, \theta, -\phi) D_{0\lambda'}^1(\phi, \theta, -\phi), \\ \lambda &= \lambda_1 - \lambda_2, \quad \lambda' = \lambda'_1 - \lambda'_2, \end{aligned} \quad (\text{A2})$$

by the usual helicity formalism.

Using the standard Dirac spinor formalism, we can also calculate Eq. (A2) at the tree level in the standard model. Specifically, we do this for the density matrix elements  $\rho_{++}, \rho_{+-}$ , and  $\rho_{-+}$  since, by CP invariance [Eq. (4.3)], we know  $T(++) = T(--)$ . We use the following results: From Auvil and Brehm,<sup>28</sup>

$$u(p, +) = \frac{1}{\sqrt{E+m}} (\not{p} + m) \begin{pmatrix} \cos\theta/2 \\ e^{i\phi} \sin\theta/2 \\ 0 \\ 0 \end{pmatrix} \quad (\text{A3a})$$

$$= \sqrt{E+m} \begin{pmatrix} \cos\theta/2 \\ e^{i\phi} \sin\theta/2 \\ \frac{p}{E+m} \begin{pmatrix} \cos\theta/2 \\ e^{i\phi} \sin\theta/2 \end{pmatrix} \end{pmatrix}, \quad (\text{A3b})$$

where the Lorentz boost is explicit in the first line, and

$$u(p, -) = \frac{1}{\sqrt{E+m}} (\not{p} + m) \begin{pmatrix} -e^{-i\phi} \sin\theta/2 \\ \cos\theta/2 \\ 0 \\ 0 \end{pmatrix} \quad (\text{A4a})$$

$$= \sqrt{E+m} \begin{pmatrix} -e^{-i\phi} \sin\theta/2 \\ \cos\theta/2 \\ \frac{p}{E+m} \begin{pmatrix} e^{-i\phi} \sin\theta/2 \\ -\cos\theta/2 \end{pmatrix} \end{pmatrix}, \quad (\text{A4b})$$

and as usual

$$u(p, \pm) \bar{u}(p, \pm) = \frac{1}{2} (\not{p} + m) (1 \pm \gamma_5 \not{\epsilon}), \quad (\text{A5})$$

$$v(p, \pm) \bar{v}(p, \pm) = \frac{1}{2} (\not{p} - m) (1 \pm \gamma_5 \not{\epsilon}), \quad (\text{A6})$$

where the *contravariant* four-vectors are

$$p^\mu = (E; p \sin\theta \cos\phi, p \sin\theta \sin\phi, p \cos\theta), \quad (\text{A7})$$

$$\epsilon^\mu = \left( \frac{p}{m}, \frac{E}{m} \hat{\mathbf{p}} \right), \quad \hat{\mathbf{p}} \equiv \mathbf{p}/|\mathbf{p}|. \quad (\text{A8})$$

For the  $Z^0$  at rest in state  $|J=1, M=0\rangle$ , we know  $\epsilon^\mu=(1,0)$ .

Remarks: (i) The  $\theta$  and  $\phi$  dependence agrees for these three density matrix elements between the results with the above spinors and that from Eq. (A2) with the  $d$  functions of Rose. (ii) Since this calculation is only to fix the phases, tricks such as setting  $r=0$  can be exploited if one already knows the magnitudes of these helicity amplitudes in the standard model. (iii) These specific positive energy spinors have been used only to calculate density matrix elements and only for amplitudes where the first particle is the fermion ( $\tau^-$  and  $e^-$ ) and the second particle is the antifermion.

In the standard model, by the above calculation we find that at the tree level the amplitudes in Eq. (A1) are those listed in Eqs. (2.2). The formation amplitudes  $\tilde{T}(s_1, s_2)$  for  $e_1^- e_2^+ \rightarrow Z^0$  then follow from Eqs. (2.2) by time reversal per Eq. (4.7).

**APPENDIX B: USAGE OF  $I(\theta_e, E_1, E_2, \phi)$  TO OBTAIN SIMPLER CORRELATION FUNCTIONS (REF. 29)**

In Sec. IV, from the full BRSC function  $I(\theta_e, \phi_e, E_1, E_2, \phi)$  listed in Eq. (4.29), we obtained  $I(\theta_e, E_1, E_2, \phi)$ . Both as a check and because it is instructive, it is useful to integrate out some of the variables to obtain simpler correlation functions.

When  $\theta_e$  and  $\phi$  are integrated out, the terms proportional to  $(1-\delta)$  and  $\alpha$  give the energy-correlation function  $I(E_1, E_2)$ , which was previously investigated in Ref. 10. On the other hand, if  $E_1, E_2,$  and  $\phi$  are integrated

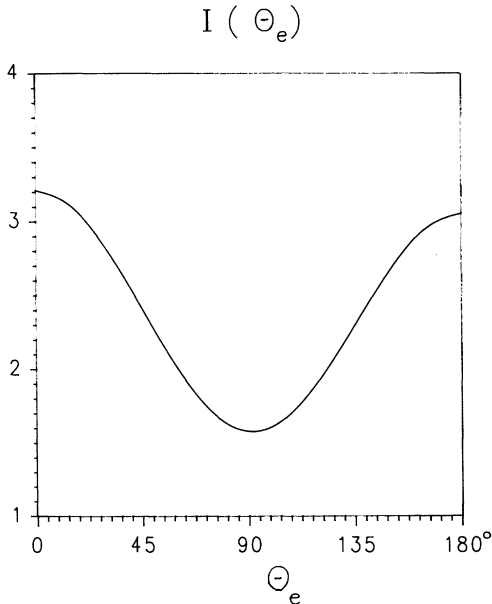


FIG. 21. Exact  $I(\theta_e)$  distribution for physical  $\tau, Z^0$ , and pion masses. To about 1% level, this is the same as the leading-order distribution of Eq. (B1).

$I(\Theta_e)$  EXACT vs L.O.  
 $m/M = 0.373 \quad \mu/m = 0.324$

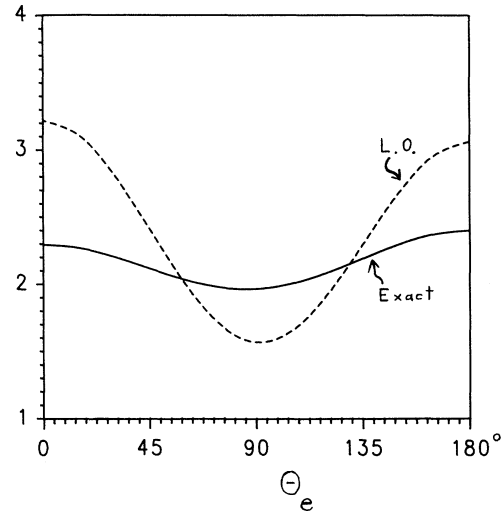


FIG. 22. Comparison of  $I(\theta_e)$  (exact) (solid curve) to  $I(\theta_e)$  (leading order) (dashed curve) for the larger  $m/M$  and  $\mu/m$  values shown. Here  $m$  is a heavy  $\tau$ , and  $\mu$  is a heavy pion, where  $M$  is a heavy  $Z$  (one of which sets the mass scale).

out, which can be done analytically using MACSYMA, one obtains the forward-backward asymmetry distribution of the  $\pi^-$  momentum vector versus the initial  $e^-$  beam momentum.

The resulting  $I(\theta_e)$  distribution is displayed in Fig. 21. To about the 1% level, this is simply the leading-order contribution.

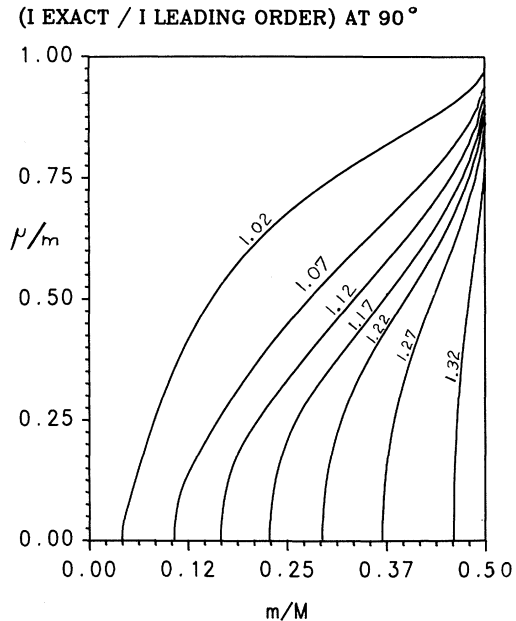


FIG. 23. Contour plot in  $m/M$  and  $\mu/m$  plane to show for what mass regions the flattening of  $I(\theta_e)$  (exact) is a sizable effect.

$$I(\theta_e)_{\text{LO}} = \frac{M^4}{4v_e^2 v_\tau^2} [(a_e^2 + v_e^2)(a_\tau^2 + v_\tau^2)(1 + \cos^2 \theta_e) + 8a_e v_e a_\tau v_\tau \cos \theta_e]. \quad (\text{B1})$$

Note that Eq. (B1) is the same as the exact tree-level  $I(\theta)$  for the unobserved process  $e^- e^+ \rightarrow \tau^- \tau^+$ , where  $\theta$  is the angle between the final  $\tau^-$  and the initial  $e^-$ . Note also that the chirality parameters  $\xi_h$  do not appear in Eq. (B1).

Analytically, Eq. (B1) can be considered as arising from an expansion of  $I(\theta_e, E_1, E_2, \phi)$  in the  $Z^0$  rest-frame variable  $\sin^2 \theta_1$ , where

$$\begin{aligned} \sin^2 \theta_1 &= \frac{1}{\gamma^2} \left[ \frac{p_1^\tau \sin \theta_1^\tau}{E_1^\tau + \beta p_1^\tau \cos \theta_1^\tau} \right]^2 + O(1/\gamma^4) \\ &= \frac{1}{\gamma^2} \left[ \frac{p_1^\tau \sin \theta_1^\tau}{E_1^\tau + \beta p_1^\tau \cos \theta_1^\tau} \right]^2 [1 + O((\mu_1/E_1)^2)], \end{aligned} \quad (\text{B2})$$

with  $\gamma = M/(2m) \approx 25.6$  for the relativistic boost  $\gamma$  between the  $Z^0$  rest frame and either of the  $\tau^\pm$  rest frames. The variables on the right-hand side of Eq. (B2) are for the  $\tau_1^-$  rest frame. In particular, we find

$$I(\theta_e, E_1, E_2, \phi) = I_0(\dots) + \sin^2 \theta_1 I_1(\dots) + O(\sin^4 \theta_1), \quad (\text{B3})$$

where

$$I_0 = \frac{\pi}{8} \left[ (1 + \cos^2 \theta_e) \mathcal{A}_0 + \frac{2T_e}{S_e} \cos \theta_e \mathcal{A}_1 \right], \quad (\text{B4})$$

$$\begin{aligned} I_1 = \frac{\pi}{16} \left[ (1 - 3 \cos^2 \theta_e) \mathcal{A}_0 - \frac{2T_e}{S_e} \cos \theta_e \mathcal{A}_1 \right. \\ \left. + (1 - 3 \cos^2 \theta_e) \kappa \sin \theta_1^\tau \sin \theta_2^\tau \cos \phi \right]. \end{aligned} \quad (\text{B5})$$

For larger values of  $\sin^2 \theta_1$ , the expansion of Eq. (B3) is not sufficient. Figure 22 shows how the asymmetry in  $\theta_e$  for the final  $\pi_1^-$  versus the incident  $e^-$  is typically reduced. This reduction is sizable when  $m/M$  and  $\mu/m$  have both increased to about  $\frac{1}{3}$ . Because of this reduction in signature, the leading-order approximation, Eq. (B1), to  $I(\theta_e)$  cannot be used indiscriminantly in considerations about new physics in the case of a decay sequence in the final state. To help in quantifying this limitation, a contour plot is presented in Fig. 23, which shows the ratio of ( $I_{\text{exact}}/I_{\text{leading order}}$ ) at  $\theta_e = 90^\circ$ . (More details are presented in Ref. 29.)

<sup>1</sup>ALEPH Collaboration, D. Decamp *et al.*, Phys. Lett. B **231**, 519 (1989).

<sup>2</sup>DELPHI Collaboration, P. Abreu *et al.*, Phys. Lett. B **231**, 539 (1989).

<sup>3</sup>L3 Collaboration, B. Adeva *et al.*, Phys. Lett. B **231**, 509 (1989).

<sup>4</sup>OPAL Collaboration, M. Z. Akrawy *et al.*, Phys. Lett. B **231**, 530 (1989).

<sup>5</sup>Results from these (Refs. 1–4) four collaborations and also from the SLAC Linear Collider (SLC) were reported in *Z Physics*, proceedings of the 25th Rencontre de Moriond, Les Arcs, France, 1990, edited by J. Tran Thanh Van (Editions Frontieres, Gif-sur-Yvette, 1990).  $\tau^- \tau^+$  pairs were first seen at the  $Z^0$  by the Mark II Collaboration, G. S. Abrams *et al.*, Phys. Rev. Lett. **63**, 724 (1989). For a review, see *Z physics at LEP I*, proceedings of the Workshop, Geneva, Switzerland, 1989, edited by G. Altarelli, R. Kleiss, and C. Verzegnassi (CERN Report No. 89-08, Geneva, 1989). For the SLC, see *Physics at the 100 GeV Mass Scale*, proceedings of the 17th SLAC Summer Institute, Stanford, California, 1989, edited by E. C. Brennan (SLAC Report No. 361, Stanford, 1990).

<sup>6</sup>ARGUS Collaboration, H. Albrecht *et al.*, Phys. Lett. B **246**, 278 (1990).

<sup>7</sup>CLEO Collaboration, M. Goldberg *et al.*, Report No. CLNS-90-99 (unpublished).

<sup>8</sup>J. M. Jowett, Report No. CERN LEP-TH/87/56 (unpublished); Report No. CERN LEP-TH/88/22 (unpublished); M. L. Perl, in *Proceedings of the Tau-Charm Factory Workshop*, Stanford, California, 1989, edited by Lydia V. Beers (SLAC Report No. 343, Stanford, 1989); R. H. Schindler, Report No. SLAC-PUB-5202, 1990 (unpublished).

<sup>9</sup>The literature on the  $Z^0 \rightarrow \tau^- \tau^+$  decay mode includes, among others, the following papers: Y.-S. Tsai, Phys. Rev. D **4**, 2821

(1971); **13**, 771 (1976); S.-Y. Pi and A. I. Sanda, Ann. Phys. (N.Y.) **106**, 171 (1977); J. Babson and E. Ma, Phys. Rev. D **26**, 2497 (1982); D. Cords *et al.*, in *Proceedings of the 3rd and Final Mark-II Workshop on SLC Physics*, Watsonville, California, 1987 (SLAC Report No. 315, Stanford, 1987); J. H. Kühn and F. Wagner, Nucl. Phys. **B236**, 16 (1984); J. Chauveau, in *Physics at LEP*, LEP Jamboree, Geneva, Switzerland, 1985, edited by J. Ellis and R. Peccei (CERN Report No. 86-02, Geneva, 1986); S. Jadach and Z. Was, Acta Phys. Pol. B **18**, 1099 (1987); F. Boillot, Ph.D. thesis, University of Paris, 1987; B. F. Ward, Phys. Rev. D **35**, 2092 (1987); **40**, 1411 (1989); F. Boillot and Z. Was, Z. Phys. C **43**, 109 (1989); K. Hagiwara, A. D. Martin, and D. Zeppenfeld, Phys. Lett. B **235**, 198 (1990); and the  $\tau$  working group report, S. Jadach and Z. Was, conveners, in *Z Physics at LEP I* (Ref. 5), Vol. 1, p. 235.

<sup>10</sup> $\tau$  spin correlations are treated using energy-correlation functions in C. A. Nelson, Phys. Rev. Lett. **62**, 1347 (1989); Phys. Rev. D **40**, 123 (1989); **41**, 2327(E) (1990); **41**, 2805 (1990).

<sup>11</sup>Usage of energy correlations at a  $\tau$ /charm factory to measure the  $\tau$  Michel parameters is discussed in *Proceedings of the Tau-Charm Factory Workshop* (Ref. 8); in particular, see J. J. Gomez-Cadenas. W. Fetscher has investigated the issue of how to determine the Lorentz structure of the purely leptonic  $\tau$  decays at  $J/\psi$ , W. Fetscher, Phys. Rev. D **42**, 1544 (1990). A. Pich has stressed the importance of data on  $\tau$  hadronic decays for understanding QCD phenomena, Valencia Report No. FTUV/89-22, 1989 (unpublished).

<sup>12</sup>The ARGUS Collaboration has very recently reported a new measurement of the  $\rho$  parameter for  $\tau$  decay,  $\rho = 0.742 \pm 0.035$  (stat)  $\pm 0.020$  (sys.), Albrecht *et al.* (Ref. 6). From  $\tau \rightarrow a_1 \nu \rightarrow (3\pi) \nu$ , they have also measured  $\xi_{a_1} = 2g_A g_V / (g_A^2 + g_V^2) = 1.14 \pm 0.34 + 0.34 / -0.17$ , Report

- No. DESY 90-079, 1990 (unpublished); see H. Kühn and F. Wagner, Nucl. Phys. **B236**, 16 (1984) and M. Feindt, Report No. DESY 90-036 (unpublished). For reviews of the known properties of the  $\tau$ , see M. L. Perl, Annu. Rev. Nucl. Part. Sci. **30**, 299 (1980); B. C. Barish and R. Stroynowski, Phys. Rep. **157**, 1 (1988); and C. Kiesling in *High Energy Electron Position Physics*, edited by A. Ali and P. Söding, *Advanced Series in Directions in High Energy Physics, Vol. 1* (World Scientific, Singapore, 1988).
- <sup>13</sup> $CP$ -violation effects in  $Z^0 \rightarrow \tau^- \tau^+$  have been investigated in the last paper of Ref. 4 and in W. Bernreuther and O. Nachtmann, Phys. Rev. Lett. **63**, 2787 (1989); W. Bernreuther, U. Low, J. P. Ma, and O. Nachtmann, Z. Phys. C **43**, 117 (1989); and J. Körner, J. P. Ma, R. Munch, O. Nachtmann, and R. Schopf, Report No. DESY 90-022, 1990 (unpublished). Investigations of  $CP$  violation with polarized  $e^-e^+$  collisions include W. B. Atwood, I. Dunietz, and P. Grosse-Wiesmann, Phys. Lett. B **216**, 227 (1989); W. B. Atwood, I. Dunietz, P. Grosse-Wiesmann, S. Matsuda, and A. I. Sanda, *ibid.* **232**, 533 (1989); and C. P. Burgess and J. A. Robinson, McGill report, 1990 (unpublished).
- <sup>14</sup> $T$ -odd effects at  $e^-e^+$  colliders have been investigated in J. F. Donoghue and G. Valencia, Phys. Rev. Lett. **58**, 451 (1987); **60**, 243(E) (1988); M. B. Gavela, F. Iddir, A. LeYaonanc, L. Oliver, O. Pène, and J. C. Raynal, Phys. Rev. D **39**, 1870 (1989); Y. Kizukuri, Phys. Lett. B **193**, 339 (1987); Y. Kizukuri and N. Oshimo, Tokai University Report No. TKU-HEP 90/01, 1990 (unpublished).  $T$ -odd effects at the  $Z^0$  have been investigated in J. Bernabeu and N. Rius, Phys. Lett. B **232**, 127 (1989).
- <sup>15</sup>See S. Jadach and Z. Was, in *Z. Physics at LEP*, (Ref. 5). For KORALZ, see S. Jadach and Z. Was, Comput. Phys. Commun. **36**, 191 (1985); and S. Jadach, B. F. L. Ward, Z. Was, R. G. S. Stuart, and W. Hollik (see Report No. CERN 89-08, Vol. 3, p. 69). Cords *et al.* (Ref. 9) cite LULEPT, D. Stoker *et al.*, Phys. Rev. D **39**, 1811 (1989). For TAUOLA, see S. Jadach, J. H. Kühn, and Z. Was, Version 1.5, Report No. CERN-TH-5856, 1990.
- <sup>16</sup>M. Jacob and G. Wick, Ann. Phys. (N.Y.) **7**, 404 (1959).
- <sup>17</sup> $CP$  Violation, edited by C. Jarlskog (World Scientific, Singapore, 1989); L. Wolfenstein, IPT Santa Barbara Report No. NSF-ITP-90-29 (1990) (unpublished); R. G. Sachs, *The Physics of Time Reversal* (University of Chicago Press, Chicago, 1987); and B. Holstein, report, 1990 (unpublished).
- <sup>18</sup>N. P. Chang and C. A. Nelson, Phys. Rev. Lett. **40**, 1617 (1978); T. L. Trueman, Phys. Rev. D **18**, 3423 (1978); and compare C. N. Yang, Phys. Rev. **77**, 242 (1950); **77**, 722 (1950). R. M. Baltrusaitis *et al.*, Phys. Rev. Lett. **52**, 2126 (1984), and D. Bisello *et al.*, Phys. Lett. B **179**, 289 (1986), determined the  $\eta_c$  to be pseudoscalar.
- <sup>19</sup>We have used  $M = 91.17 \text{ GeV}/c^2$  for the  $Z^0$  mass,  $m = 1.7841 \text{ GeV}/c^2$  for the  $\tau$  mass, and  $\sin^2\theta_W = 0.23$ . Note that in this paper when we integrate out angular variables in passing from one correlation function  $I(\dots)$  to another, we do not keep the overall  $2\pi$ , etc., normalization factors so as to simplify the listed formulas.
- <sup>20</sup>Our treatment of ideal statistical errors is as in the second paper of Ref. 10.
- <sup>21</sup>The kinematics of the  $X \rightarrow \tau^- \tau^+ \rightarrow A^- B^+ X$  final state, including the twofold ambiguity in the  $\tau_1^-$  momentum direction, was treated earlier in J. R. Dell'Aquila and C. A. Nelson, Nucl. Phys. **B320**, 86 (1989); C. A. Nelson, Report No. SUNY BING 10/15/88 (unpublished).
- <sup>22</sup>A. De Rujula and R. Rückl, in *Proceedings of the CERN-ECFA Workshop on Feasibility of Hadron Colliders in the LEP Tunnel*, Lausanne, Switzerland, 1984 (CERN Report No. 84-10/ECFA Report No. 84/85, Geneva, 1984), p. 571.
- <sup>23</sup>K. Winter, Report No. CERN-EP/89-182, 1989 (unpublished).
- <sup>24</sup>M. E. Rose, *Elementary Theory of Angular Momentum* (Wiley, New York, 1957).
- <sup>25</sup>K. G. Hayes and M. L. Perl, Phys. Rev. D **38**, 3351 (1988); Particle Data Group, G. P. Yost *et al.*, Phys. Lett. B **204**, 1 (1988).
- <sup>26</sup>K. K. Gan and M. L. Perl, Int. J. Mod. Phys. A **3**, 531 (1988).
- <sup>27</sup>The  $H$  subscript on  $\alpha$  has been suppressed elsewhere in this paper, except in Table V. It denotes the fact that  $\alpha_H$  can be determined from the harder lepton's energy spectrum in  $Z^0 \rightarrow \tau^+ \tau^- \rightarrow \mu^+ \mu^- X$  (see first paper in Ref. 10).
- <sup>28</sup>R. D. Auvil and J. J. Brehm, Phys. Rev. **145**, 1152 (1966).
- <sup>29</sup>S. Goozovat, Master's thesis, State University of New York, Binghamton, 1990.